

NAD⁺-NADH modelling studies : an enzymatic and chemical approach

Citation for published version (APA):

Beijer, N. A. (1990). *NAD⁺-NADH modelling studies : an enzymatic and chemical approach*. [Phd Thesis 1 (Research TU/e / Graduation TU/e), Chemical Engineering and Chemistry]. Technische Universiteit Eindhoven. <https://doi.org/10.6100/IR342323>

DOI:

[10.6100/IR342323](https://doi.org/10.6100/IR342323)

Document status and date:

Published: 01/01/1990

Document Version:

Publisher's PDF, also known as Version of Record (includes final page, issue and volume numbers)

Please check the document version of this publication:

- A submitted manuscript is the version of the article upon submission and before peer-review. There can be important differences between the submitted version and the official published version of record. People interested in the research are advised to contact the author for the final version of the publication, or visit the DOI to the publisher's website.
- The final author version and the galley proof are versions of the publication after peer review.
- The final published version features the final layout of the paper including the volume, issue and page numbers.

[Link to publication](#)

General rights

Copyright and moral rights for the publications made accessible in the public portal are retained by the authors and/or other copyright owners and it is a condition of accessing publications that users recognise and abide by the legal requirements associated with these rights.

- Users may download and print one copy of any publication from the public portal for the purpose of private study or research.
- You may not further distribute the material or use it for any profit-making activity or commercial gain
- You may freely distribute the URL identifying the publication in the public portal.

If the publication is distributed under the terms of Article 25fa of the Dutch Copyright Act, indicated by the "Taverne" license above, please follow below link for the End User Agreement:

www.tue.nl/taverne

Take down policy

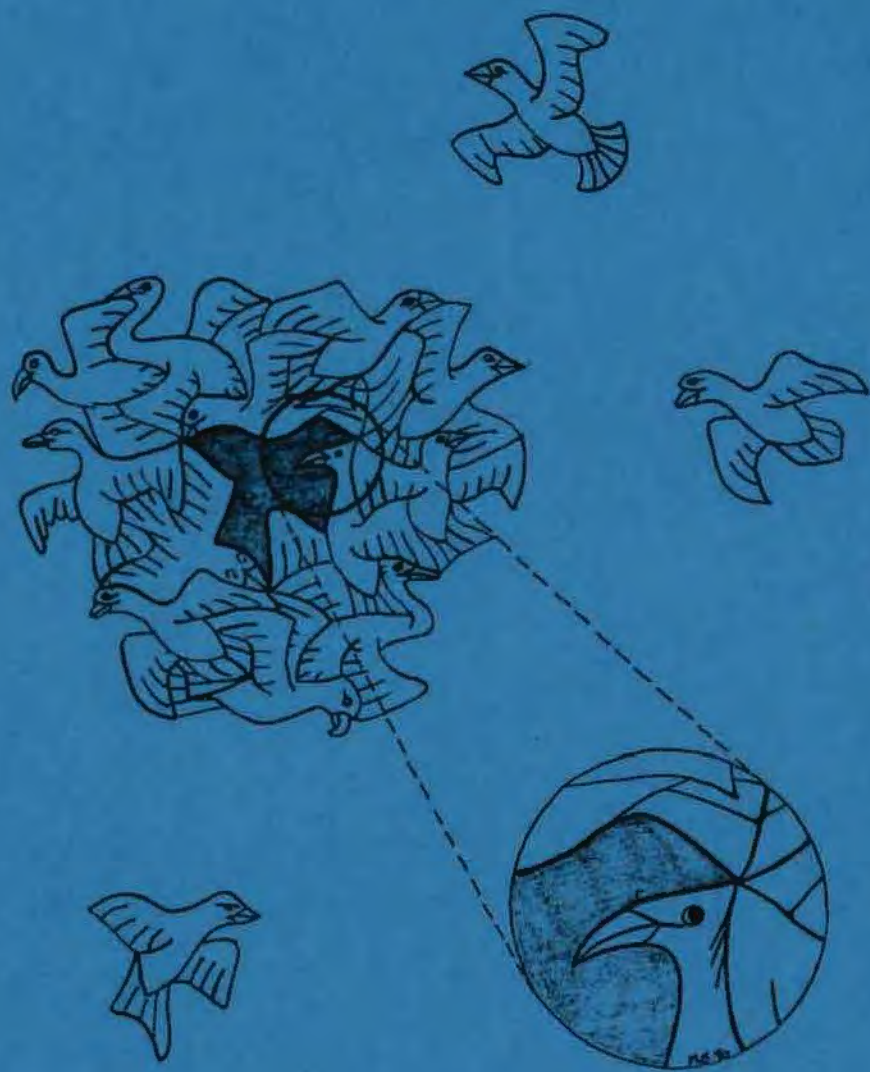
If you believe that this document breaches copyright please contact us at:

openaccess@tue.nl

providing details and we will investigate your claim.

NAD⁺-NADH MODELLING STUDIES

AN ENZYMATIC AND CHEMICAL APPROACH



NICOLINE A. BEIJER

NAD⁺-NADH MODELLING STUDIES

**AN ENZYMATIC AND
CHEMICAL APPROACH**

NAD⁺-NADH MODELLING STUDIES

AN ENZYMATIC AND CHEMICAL APPROACH

Proefschrift

ter verkrijging van de graad van doctor aan
de Technische Universiteit Eindhoven, op gezag
van de Rector Magnificus, prof. ir. M. Tels, voor
een commissie aangewezen door het College
van Dekanen in het openbaar te verdedigen op
vrijdag 7 december 1990 om 16.00 uur

door

NICOLINE ANNETTE BELJER

geboren te Geldrop

**Dit proefschrift is goedgekeurd
door de promotoren:**

Prof. Dr. E.M. Meijer

en

Prof. Dr. R.M. Kellogg

Omslag:

**geïnspireerd door Eschers werk en
dit promotieonderzoek (NAB).**

Aan mijn ouders

CONTENTS

ABBREVIATIONS	v
1 INTRODUCTION	1
1.1 Coenzyme dependent enzymes and their limitations in preparative use	1
1.2 Nicotinamide Adenine Dinucleotide (NAD ⁺ -NADH)	2
1.3 Chemical NADH model systems	5
1.4 Enzymatic studies	6
1.5 Outline of this thesis	8
References	8
2 STEREOSELECTIVE REDUCTION OF BENZOIN BY THE NADH MODEL 3-(N,N-DIMETHYLCARBAMOYL)-1,2,4-TRIMETHYL-1,4-DIHYDRO- PYRIDINE	11
Abstract	11
2.1 Introduction	12
2.2 Experimental	13
2.3 Results and discussion	14
2.4 Conclusions	16
References	17
3 MODELLING OF NAD⁺ AND NAD⁺ ANALOGUES IN HLADH USING MOLECULAR MECHANICS	19
Abstract	19
3.1 Introduction	20
3.2 The AMBER model	21
3.2.1 Introduction	21
3.2.2 Starting geometries	22
3.2.2.1 Enzyme	22

3.2.2.2	Coenzyme	23
3.2.2.3	DMSO	24
3.2.2.4	Zinc	24
3.2.3	Results and discussion	24
3.2.3.1	NAD ⁺ geometry	24
3.2.3.2	NAD ⁺ analogue geometry	30
3.3	Refinement of the AMBER model describing the "out-of-plane" orientation	33
3.3.1	Introduction	33
3.3.2	Parameters for the "out-of-plane" orientation	34
3.3.3	Results and discussion	35
3.4	Conclusions	37
	References	37
4	RELATIONSHIP BETWEEN REACTIVITIES AND SIMULATED CONFORMATION OF NAD⁺ AND NAD⁺ ANALOGUES	41
	Abstract	41
4.1	Introduction	42
4.2	Materials and methods	43
4.2.1	Enzyme kinetics	43
4.2.2	Procedure for calculational studies	43
4.3	Results and discussion	44
4.3.1	Molecular mechanics calculations	44
4.3.2	Kinetic studies	48
4.3.3	Discussion	48
4.4	Conclusions	50
	References	51
5	MIMICKING THE CONFORMATIONAL CHANGES OF HLADH UPON BINDING OF NAD⁺ AND NAD⁺ FRAGMENTS	53
	Abstract	53
5.1	Introduction	54
5.2	Procedure for calculational studies	55

5.3	Results and discussion	56
5.3.1	Binding of NAD ⁺	56
5.3.2	Binding of NAD ⁺ fragments	58
5.4	Conclusions	60
	References	61
6	SIMULATION OF POLYETHYLENE GLYCOL BOUND NAD⁺	63
	Abstract	63
6.1	Introduction	64
6.2	Procedure for calculational studies	65
6.3	Results and discussion	65
6.4	Conclusions	68
	References	68
7	SIMULATION OF THE COENZYME GEOMETRY IN HLADH WITH SINGLE AMINO ACID SUBSTITUTIONS	71
	Abstract	71
7.1	Introduction	72
7.2	Procedure for calculational studies	72
7.3	Results and discussion	73
7.3.1	Substitution of Val 203	73
7.3.2	Substitution of His 51	75
7.3.3	Substitution of Glu 68	76
7.3.4	Simulation of other single amino acid substitutions in HLADH	78
7.4	Conclusions	81
	References	81
	APPENDIX A	83
	APPENDIX B	85

SUMMARY	87
SAMENVATTING	89
CURRICULUM VITAE	92
NAWOORD	93

ABBREVIATIONS

ac ³ PdAD ⁺ /ac ³ PdADH	3-acetylpyridine adenine dinucleotide and its reduced form
AMP	adenosine monophosphate
clac ³ PdAD ⁺	3-chloroacetylpyridine adenine dinucleotide
cn ³ PdAD ⁺	3-cyanopyridine adenine dinucleotide
DMSO	dimethyl sulfoxide
fPdAD ⁺ /fPdADH	3-formylpyridine adenine dinucleotide and its reduced form
GAPDH	glyceraldehyde-3-phosphate dehydrogenase
HLADH	horse liver alcohol dehydrogenase
LDH	lactate dehydrogenase
m ⁴ NAD ⁺	4-methylnicotinamide adenine dinucleotide
NAD ⁺ /NADH	nicotinamide adenine dinucleotide and its reduced form
NMN ⁺	nicotinamide mononucleotide
NR ⁺	nicotinamide ribose
PdAD ⁺	pyridine adenine dinucleotide
PEG-NAD ⁺	polyethylene glycol bound NAD ⁺
pp ³ PdAD ⁺	3-propionylpyridine adenine dinucleotide
sNAD ⁺ /sNADH	thionicotinamide adenine dinucleotide and its reduced form
TMS	tetramethyl silane
AMBER	assisted model building with energy refinement
MNDO	minor neglect of differential overlap program
NMR	nuclear magnetic resonance
RMS	root mean square
UV/VIS	ultraviolet/visible light

Abbreviations for amino acids are in accord with recommendations of the IUPAC-IUB Commission on Biochemical Nomenclature (Eur. J. Biochem. 138 (1984), 9-37).

CHAPTER 1

INTRODUCTION

1.1 Coenzyme dependent enzymes and their limitations in preparative use

Syntheses of optically pure compounds have become of major importance in recent years. Enzymes present unique opportunities in this regard, because they are usually very selective and show high efficiency and activity under mild conditions. Of all known enzymes approximately 40% require coenzymes for catalytic activity. So far the number of successful applications of enzymes that depend on the coenzyme nicotinamide adenine dinucleotide (NAD^+) is limited. One fundamental obstacle to the large-scale use of

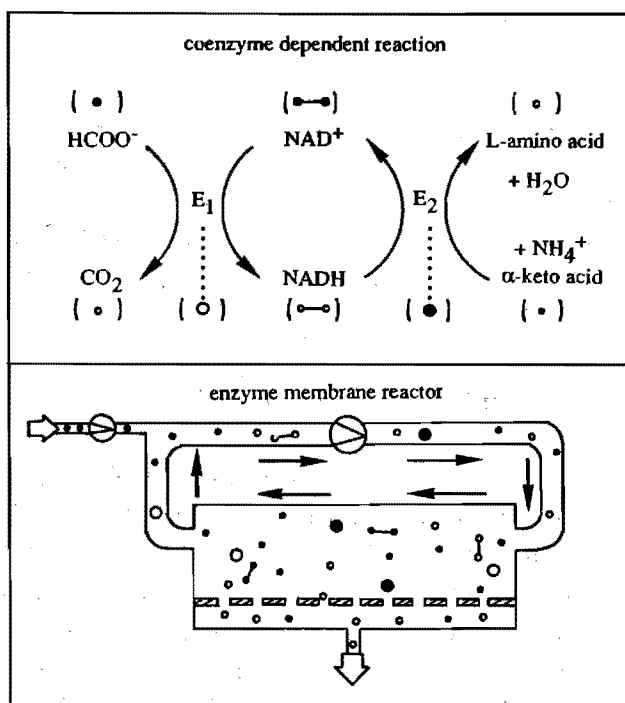


Figure 1.1 Enzyme membrane reactor concept for continuous enzymatic synthesis with coenzyme regeneration [1].

NAD⁺-dependent enzymes has been the expense of the cofactor. Nicotinamide cofactors cost too much to be used as stoichiometric reagents for other than small-scale synthesis. If NAD⁺-dependent enzymes are to be employed as catalysts for preparative chemistry, effective methods for cofactor retention and regeneration must be available.

Due to its relatively small size, retention might be difficult. A means to overcome this problem is to enlarge the coenzyme to a size such that it is separable from the products.

One of the systems investigated is the enzyme membrane reactor developed by Wandrey and co-workers [1-3]. Continuous production of L-amino acids from the corresponding α -keto acids by stereospecific reductive amination has been achieved with little cofactor consumption in a membrane reactor in which NAD⁺ is covalently linked to polyethylene glycol (figure 1.1).

For coenzyme regeneration, the essential factor is to employ a cheap regeneration substrate that offers no by-products or at most a by-product that neither interferes with nor causes problems during separation [4]. The enzymatic oxidation of formate to CO₂ by formate dehydrogenase offers a favourable method for the regeneration of NADH. In this way product isolation is simplified [1].

Although much research is in progress for increasing the use of NAD⁺-dependent enzymes, up till now no clear insight has been obtained into the relationship between structure and function of enzyme and coenzyme, i.e., no systematic explanation and interpretation of activity and stereospecificity have been provided so far.

The use of simpler coenzyme analogues is another way to overcome the high NAD⁺ costs. For a rational design of such new coenzyme derivatives, fundamental insight into the structure-function relationship of coenzyme and enzyme is again essential.

1.2 Nicotinamide Adenine Dinucleotide (NAD⁺-NADH)

NAD⁺ is a coenzyme that takes part in numerous cellular processes, particularly in the intermediary metabolism and in energy-conversion reactions, e.g., electron transport and oxidative phosphorylation [5-8]. In combination with specific enzymes (dehydrogenases) the coenzyme is involved in the dehydrogenation of many substrates. During this reaction NAD⁺ undergoes reduction, in which the nicotinamide ring accepts a hydride ion to yield the dihydropyridine form (NADH). Vennesland and Westheimer [9] established, with deuterium labeled substrates, that the reactions catalyzed by NAD⁺-dependent enzymes exhibit regio- and stereospecificity with respect to substrate

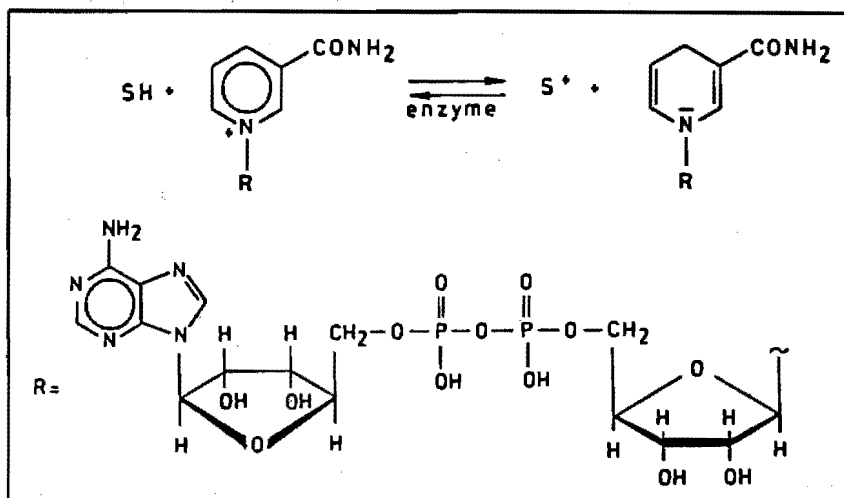


Figure 1.2 Schematic representation of the enzymatic reduction of NAD⁺ to NADH with a substrate (SH).

and coenzyme. It has become increasingly evident that this aspect is one of the most stringently conserved properties of NAD⁺-dependent oxidoreductases [8].

The stereochemical course of the hydride transfer is dictated by the enzyme. Depending on the enzyme type (A- or B-specific enzymes), either hydrogen atom H_A or atom H_B can be transferred, as illustrated in figure 1.3.

This H_A and H_B stereospecificity is on the one hand the result of one-sided shielding by the enzyme, on the other hand the result of the relative orientation of the pyridinium ring and the carboxamide side chain in the active site of the enzyme. The relevance of the CONH₂ group to the kinetics in the enzyme-catalyzed stereospecific hydride transfer has been discussed by Dutler [10]. He envisaged that the pyridine ring has enough freedom of motion to change its position during the hydrogen transfer, a movement possibly accompanied by the rotation of the CONH₂ group out of the plane of the pyridine ring.

The stereospecificity arises in the positioning of the nicotinamide moiety with respect to the substrate as soon as a complex with the enzyme is formed. The CONH₂ group loses its rotational freedom by formation of hydrogen bonds with the surrounding amino acids. When the CONH₂ group is fixed, and this will be in an orientation rotated out of the pyridine plane ("out-of-plane" orientation), migration of either H_A or H_B is favoured, depending on the type of enzyme. This causes the reaction to be effectively stereospecific.

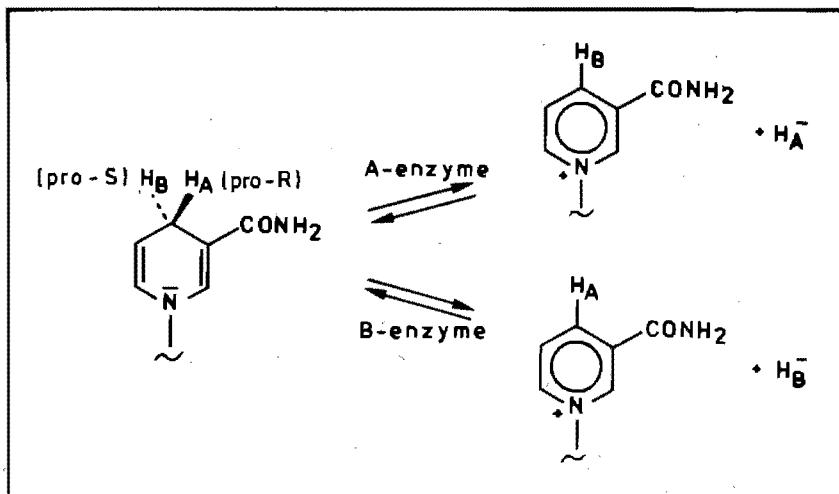


Figure 1.3 Stereospecific hydride transfer by A- and B-specific dehydrogenases.

The basic idea of the carboxamide "out-of-plane" orientation as outlined in the foregoing originates from Donkersloot and Buck [11]. They found, based on quantum chemical calculations, that the enthalpy of the transition state of the hydride transfer is lowered when the carboxamide group is rotated out of the pyridinium plane. These theoretical studies suggest that the carboxamide oxygen is orientated *syn* with respect to the hydride transfer direction (figure 1.4). This implies that the amide carbonyl dipole is

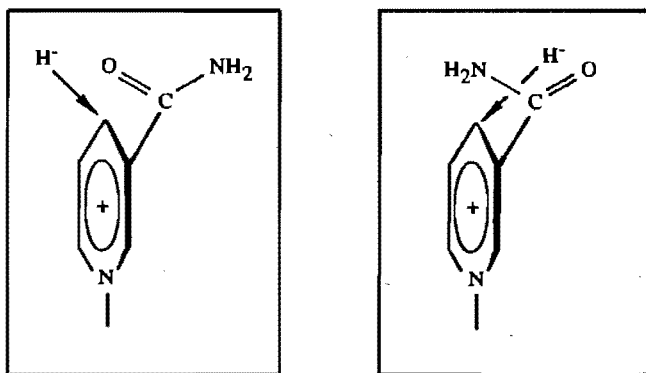


Figure 1.4 Representation of the entry of the hydride ion in the direction of the carbonyl group (A- and B-specificity).

directed to the substrate. On the strength of these calculations it is assumed that also in enzymatic circumstances the "out-of-plane" orientation of the carboxamide group is a dominant factor in determining the rate of stereoselective hydride transfer. This idea of *syn* "out-of-plane" is supported by röntgen crystallographic data. The X-ray structure of the ternary complex of NAD⁺, dimethylsulfoxide (DMSO) and the A-specific enzyme horse liver alcohol dehydrogenase (HLADH) elucidated by Eklund et al. [12] (2.9 Å resolution, crystallographic R factor of 0.22) showed an 30° "out-of-plane" rotation. The B-side of the nicotinamide group is shielded by the hydrophobic wall of the cleft, whereas the A-side is directed towards the substrate. Skarzynski and co-workers [13] found in their high resolution crystallographic study of a binary complex of NAD⁺ and the B-specific glyceraldehyde-3-phosphate dehydrogenase (GAPDH) from *Bacillus stearothermophilus* (1.8 Å resolution, crystallographic R factor of 0.177) that the amide group was rotated 22° out of the pyridinium plane. Again the carbonyl dipole is directed towards the substrate binding region, this time favouring the B-specific hydride transfer process.

1.3 Chemical NADH model systems

Insight into the enzymatic mechanism can be gained with the aid of synthesized model systems designed on the concept of the working mechanism of the enzymes.

For more than a decade, efforts have been made to create model compounds mimicking the activity of the NAD⁺-dependent enzymes in the hope of shedding light on the stereochemical picture of the hydride transfer *in vivo*. The development of an efficient NADH mimic have ranged through a host of structurally diverse 1,4-dihydropyridines with varying degrees of success [14-19].

NADH model systems not only give more insight into the enzymatic working mechanism, but they can also be used as efficient catalysts in the stereospecific reduction of prochiral substrates to obtain optically active products, which are becoming more and more important. Numerous asymmetric reductions by such compounds have already been reported [14-19].

In this study the concept of the carbonyl "out-of-plane" mediated stereochemical hydride uptake as proposed by Donkersloot and Buck is verified experimentally using a NADH model compound. The NADH model used requires the carboxamide group to be forced out of the pyridine plane, which is achieved by the steric hindrance of neighbouring methyl groups on the pyridine ring in order to simulate either H_A or H_B reactivity. Two types of stereospecificity need to be considered; on the one hand the A- or B-specificity of

the coenzyme, on the other hand the chirality of the alcohol produced by the reduction of an asymmetric ketone by the NADH model.

1.4 Enzymatic studies

Over the last decade, the interaction of NAD^+ with dehydrogenases has been studied extensively in an attempt to understand the factors involved in the productive binding between NAD^+ and the enzyme. However up till now the insight into the relation between structure and function of enzyme and coenzyme is still not profound.

In our study the binding of NAD^+ in HLADH is analyzed. This enzyme has been used because much is known, such as kinetic and X-ray data of the ternary complex HLADH, NAD^+ and the substrate analogue DMSO. This X-ray structure of the ternary complex, elucidated by Eklund and co-workers [12], is the starting point for the study in this thesis.

HLADH is one of the most well documented NAD^+ -dependent enzymes (see for example [12,20-23]). It is an A-specific enzyme that catalyzes the oxidation of various primary and secondary alcohols to the corresponding aldehydes and ketones.

HLADH is a dimer of two identical subunits, each subunit (374 amino acids) divided into two distinct domains [12,21]. One is used for coenzyme binding and the second domain provides residues necessary for substrate binding and catalytic action. HLADH carries two firmly bound zinc ions, one of which, the active site zinc ion, is essential for the oxidation-reduction reactions. A schematic structure of HLADH is depicted in figure 1.5.

HLADH binds NAD^+ in such a way that the pyridinium ring interacts on one side with the residues Thr 178, Val 203 and Val 294, through which the B-specific side of the enzyme is shielded and the carboxamide group is directed toward the substrate, establishing the A-specificity of the enzyme. The carboxamide side chain is then fixed by three amino acid residues; the oxygen atom of the carboxamide is hydrogen bonded to the main chain nitrogen atom of Phe 319 and the amino group is hydrogen bonded to the carbonyl oxygens of Val 292 and Ala 317 [22,23].

Additionally, it is known that the NAD^+ binding domains of different dehydrogenases are closely related in structure and bind the coenzyme in a similar way as HLADH [22].

In order to obtain fundamental insight into the relationship between structure and function of NAD^+ and the enzyme, not only NAD^+ but also NAD^+ analogues should be analyzed in their interaction with the enzyme. Although some kinetic data for the enzyme catalyzed reactions with NAD^+ analogues are known, interpretation in terms of coenzyme geometries in the active site remain speculative.

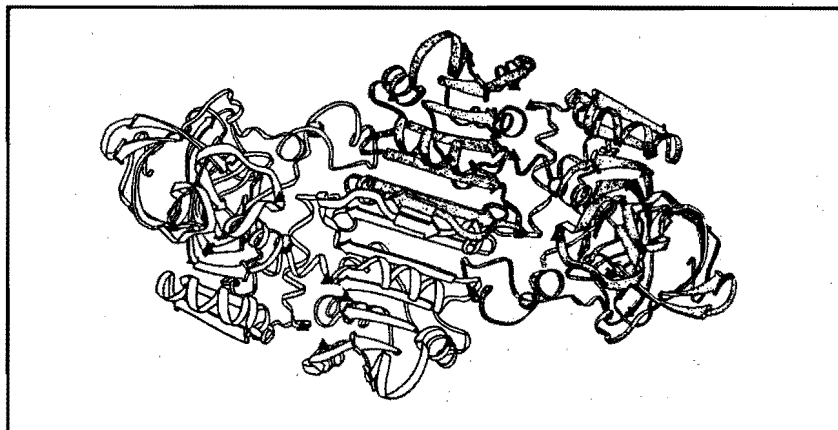


Figure 1.5 Schematic diagram of the HLADH dimer [21].

We simulated NAD^+ and NAD^+ analogues in the active site of HLADH using AMBER (= Assisted Model Building with Energy Refinement) molecular mechanics calculations in order to evaluate essential interactions between enzyme and the coenzyme.

It is known that dehydrogenases exhibit a conformational change on binding of the coenzyme [12,20-23]. This has also been examined by studying NAD^+ fragments.

As mentioned earlier, retention of NAD^+ in preparative use has been successfully employed by Wandrey et al. [1-3] using polyethylene glycol bound NAD^+ in the enzyme membrane reactor. Using molecular mechanics we simulated the geometry of PEG- NAD^+ in the active site of HLADH in order to rationalize its activity.

Although the major part of this thesis is focussed on modelling of the coenzyme, the relation between enzyme and coenzyme can also be elucidated by modifying the enzyme structure in its active site. Important amino acids can be distinguished by modelling through selective altering of the amino acids in the enzyme active site and studying its influence on the coenzyme geometry. Possibly an even better interaction can be obtained between enzyme and coenzyme. The methodology developed may be used as a basis for future protein engineering of HLADH.

In summary, on the one hand this study of the structure-function relationship of enzyme and coenzyme can lead to a straightforward synthesis of active NAD^+ analogues, on the other hand the methodology developed can be used to select targets for site-directed mutagenesis in order to engineer genetically HLADH so as to optimize the interaction of the apo-enzyme and coenzyme analogues.

1.5 Outline of this thesis

This thesis describes a chemical and enzymatic study of the coenzyme couple NAD^+ -NADH. The main aim of this investigation is to improve the fundamental insight into the coenzyme-enzyme interactions.

Chapter 2 presents the stereochemical course of the reduction of the α -hydroxy ketone benzoin with a NADH model compound. The importance of the "out-of-plane" rotation is highlighted.

A molecular mechanics method has been developed in chapter 3 starting from the X-ray ternary complex of HLADH, NAD^+ and DMSO in order to simulate the geometry of NAD^+ and NAD^+ derivatives (modified in the pyridinium side chain) in the active site.

In chapter 4 the enzymatic activity of NAD^+ and NAD^+ analogues with HLADH is rationalized by their conformation in the active site determined with the AMBER molecular mechanics model.

Chapter 5 describes the simulation of conformational changes in HLADH after binding of NAD^+ and some NAD^+ fragments.

In chapter 6 we report that the AMBER model enables us to rationalize the enzymatic activity of the commercially applied polyethylene glycol bound NAD^+ .

The methodology developed has been extended to enzyme modifications (amino acid substitutions in HLADH) as a first step on the way to optimize the enzyme-coenzyme interactions. In chapter 7 some preliminary results are discussed.

References

1. Wichmann, R., Wandrey, C., Bückmann, A.F. and Kula, M.R. *Biotechn. and Bioeng.* 23 (1981), 2789-2802.
2. Wandrey, C. and Wichmann, R. *Biotechn. Series 5* (1985), 177-208.
3. Wandrey, C. in "Proceedings 4th European Congress on Biotechnology" (O.M. Neijssel, R.R. van der Meer and K.Ch.A.M. Luyben, eds.), Elsevier, Amsterdam, 4 (1987), 171-188.
4. Chenault, H.K. and Whitesides, G.M. *Appl. Biochem. Biotechn.* 14 (1987), 147-197.
5. Colowick, S.P., Van Eys, J. and Park, J.M. *Comp. Biochem.* (Florkin and Stolz, eds) 14 (1966), 1-98.
6. Sund, H. and Theorell, H. in "The enzymes" (P.D. Boyer, H. Lardy and K. Myrback, eds) 2d ed., Academic Press, New York and London, 7 (1962), 25-83.

7. Sund, H. in "Pyridine Nucleotide-dependent Dehydrogenases" (H. Sund, ed.), de Gruyter, Berlin, W. Germany (1977).
8. You, K.S. *Crc. Crit. Rev. Biochem.* 17 (1984), 313-451.
9. Vennesland, B. and Westheimer, F.H. in "The mechanism of enzyme action" (W.D. McElroy and B. Glass, eds) John Hopkins Press, Baltimore, (1954).
10. Dutler, H. in "Pyridine Nucleotide-dependent Dehydrogenases" (H. Sund, ed.), de Gruyter, Berlin, W. Germany, (1977), 325.
11. Donkersloot, M.C.A. and Buck, H.M. *J. Am. Chem. Soc.* 103 (1981), 6554-6558.
12. Eklund, H., Samama, J.P. and Jones, T.A. *Biochemistry* 23 (1984), 5982-5996.
13. Skarzynski, T., Moody, P.C.E. and Wonacott, A.J. *J. Mol. Biol.* 193 (1987), 171-187.
14. Ohnishi, Y., Kagami, M. and Ohno, A. *J. Am. Chem. Soc.* 97 (1975), 4766-4768.
15. Endo, T., Hayashi, Y. and Okawara, M. *Chem. Lett.* (1977), 391.
16. Ohno, A.J., Ikeguchi, M., Kimura, T. and Oka, S. *J. Am. Chem. Soc.* 101 (1979), 7036-7040.
17. de Kok, P.M.T., Ph. D. Thesis, Eindhoven University of Technology (1988).
18. Inouye, Y., Oda, J. and Baba, N. in "Asymmetric Synthesis" (J.D. Morrison, ed.), Academic press, London, 2 (1983), 91-124.
19. Meijers, A.I. and Oppenlaender, T. *J. Am. Chem. Soc.* 108 (1986), 1989-1996.
20. Eklund, H., Samama, J.P., Wallén, L., Brändén, C.I., Åkeson, Å. and Jones, T.A. *J. Mol. Biol.* 146 (1981), 561-587.
21. Biellmann, J.F. *Acc. Chem. Res.* 19 (1986), 321-328.
22. Eklund, H. and Brändén, C.I. in "Coenzymes and Cofactors, Pyridine Nucleotide coenzymes" (D. Dolphin, O. Avramovic and R. Poulson, eds), John Wiley and Sons, New York, 2A (1987), 51-98.
23. Eklund, H. and Brändén, C.I. *Biological Macromolecules and Assemblies* (1987), 73-142.

CHAPTER 2*

STEREOSELECTIVE REDUCTION OF BENZOIN BY THE NADH MODEL 3-(N,N-DIMETHYLCARBAMOYL)-1,2,4-TRIMETHYL-1,4-DIHYDROPYRIDINE

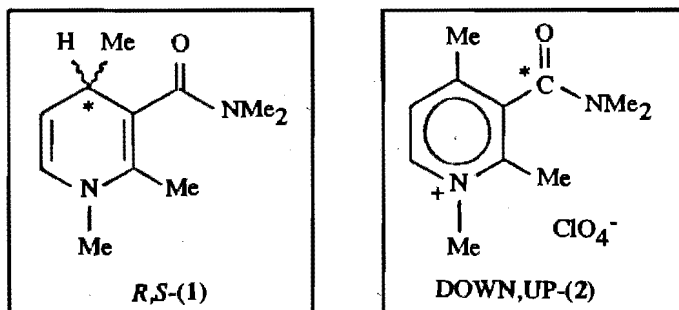
Abstract

The $\text{Mg}(\text{ClO}_4)_2$ -induced reduction of racemic benzoïn by the racemic NADH model compound 3-(N,N-dimethylcarbamoyl)-1,2,4-trimethyl-1,4-dihydropyridine (1) leads - in accordance to Cram's rule - exclusively to *meso*-1,2-diphenyl-1,2-ethanediol. On the other hand *R*-(1) also reduces *S*-benzoïn to yield *meso*-1,2-diphenyl-1,2-ethanediol, but *S*-(1) is reluctant to react with *S*-benzoïn. A strictly organized intermediate, composed of chelated substrate, dihydropyridine and magnesium ion is involved on the path to the transition state.

* N.A. Beijer, J.A.J.M. Vekemans and H.M. Buck, *Recl. Trav. Chim. Pays-Bas* 109 (1990), 434-436.

2.1 Introduction

Recently it has been shown that the NADH model compound 3-(*N,N*-dimethylcarbamoyl)-1,2,4-trimethyl-1,4-dihydropyridine (1) combines high reactivity with excellent asymmetric induction [1].



The induction of chirality in the reduction of carbonyl compounds has been studied extensively [1-4]. We proposed a mechanism in which a strictly organized transition state intervenes, i.e., the amide carbonyl dipole of the dihydropyridine system is rotated out of the pyridine plane with the amide oxygen atom facing the substrate (the migrating hydride and the amide carbonyl dipole are *syn*-oriented). A magnesium ion plays a crucial role in inducing both high stereoselectivity and high reactivity. It acts as a Lewis acid which coordinates the substrate and hydride donor with concomitant *syn* "out-of-plane" rotation of the amide carbonyl dipole. The conformation of the resulting axial chiral pyridinium cation (2) (CO up or CO down) has been correlated with the *S*- and *R*-configurations of (1). This unambiguously demonstrated that, in the complex, the migrating hydride and the amide CO dipole are *syn* oriented [5-12].

The successful stereoselective reduction of several prochiral carbonyl substrates, e.g., methyl benzoylformate, by (1) [1], prompted us to extend our investigations to the stereoselective reduction of prochiral compounds. The reaction of (1) with benzoin, an α -hydroxy ketone, has been investigated. We will show that, independent of the enantiomeric composition of either benzoin or (1), *meso*-1,2-diphenyl-1,2-ethanediol (*meso*-hydrobenzoin) is exclusively formed.

2.2 Experimental

NMR spectra were run on a Bruker AC200 spectrometer (^1H NMR at 200 MHz and ^{13}C NMR at 50.3 MHz) using TMS as internal standard.

3-(*N,N*-Dimethylcarbamoyl)-1,2,4-trimethyl-1,4-dihydropyridine (1) was synthesized in a few steps as outlined previously [1]. Enantiomeric separation of (1) was accomplished chromatographically on a 100 mg scale on cellulose triacetate (Merck, 25 x 40 μm) upon elution with isopropanol. A ^1H NMR study using (+)-Eu(hfc)₃ as shift reagent was applied to determine the enantiomeric excess of the enantiomer predominantly present.

Racemic benzoin (39.6 mg) was reduced, during 1 h, by 35 mg racemic dihydropyridine (1) in CD_3CN (0.4 ml) in the presence of an equivalent amount of magnesium perchlorate at 0°C. The organic solvent was removed *in vacuo* at room temperature and the residue was partitioned between aqueous NH_4Cl (4 ml 0.1 M) and CH_2Cl_2 (8 ml).

The organic phase was washed with water (2 x 1 ml), dried (MgSO_4) and concentrated. The solid residue was purified by chromatography (silica gel, Merck, 0.063-0.200 mm, 2 g) via elution with ethyl acetate-dichloromethane (1:7) to give *meso*-1,2-diphenyl-1,2-ethanediol (R_f 0.3).

^1H NMR (CD_3CN) for benzoin: δ 4.5 (s,1H,OH), 6.1 (s,1H,H), 7.2-8.1 (m,10H,Ph); *meso*-hydrobenzoin: δ 3.3-3.4 (s,2H,OH), 4.6-4.7 (s,2H,H), 7.2 (s,10H,Ph) and (*S,S*)(-)-hydrobenzoin: δ 3.7-3.8 (s,2H,OH), 4.5-4.6 (s,2H,H), 7.2 (s,10H,Ph); ^{13}C NMR (CD_3CN) for *meso*-hydrobenzoin: δ 78.3, 118.3, 128.1, 128.5, 142.7 and (*S,S*)(-)-hydrobenzoin: δ 79.3, 118.3, 128.2, 128.6, 142.7.

m.p. *meso*-hydrobenzoin 133-135°C (specified for the commercial Aldrich products: *meso* 137-139°C; (*S,S*)(-) 148-150°C).

The combined aqueous layers were evaporated below 30°C at low pressure. The residue was suspended in CH_3CN and the filtrate was concentrated to give the pyridinium perchlorate (2) (contaminated with some inorganic salt) [1].

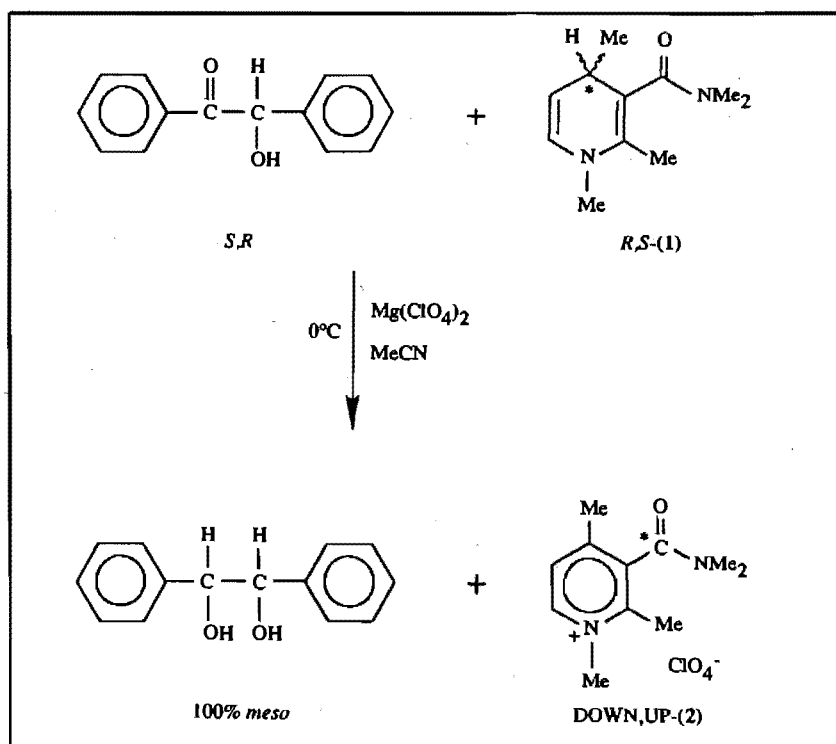
The remaining reactions were carried out in a manner similar to the above described.

The enantiomeric excess starting with optically (1) was established using (+)-Eu(hfc)₃ in CD_3CN to separate the *syn* and *anti* N-Me proton signals. The routine integration and the glinfit method (Glinfit program, Copyright Bruker Spectrospin AG, Switzerland) (rms < 4%) was used to establish the enantiomeric excess.

2.3 Results and discussion

It was observed that the dihydropyridine (1) was able to reduce benzoin in acetonitrile in the presence of magnesium perchlorate (Scheme 2.1). The reaction products were separated by partitioning between CH_2Cl_2 (1,2-diphenyl-1,2-ethanediol) and water (pyridinium perchlorate).

Scheme 2.1 Reduction of benzoin with the NADH model compound (1).



^1H and ^{13}C NMR spectra of the diol in CD_3CN before and after chromatographic purification indicated the exclusive presence of the *meso*-diastereoisomer [4]. The pyridinium perchlorate (2), derived from optically active (1), was obtained in high enantiomeric excess.

Table 2.I Stereoselective reduction of benzoin^a with the 1,4-dihydropyridine *R*-(1) and *S*-(1) in the presence of Mg(ClO₄)₂ at 0°C.

entry	dihydropyridine (1)		benzoin	<i>meso</i> -diol	pyridinium (2)	
	confign	ee(%) ^b	confign	yield ^c	confor	ee(%)
1	rac.	-	rac.	100	rac	-
2	R	96	S	95	DOWN	97
3	S	96	S	2	UP	65 ^d
4	R	65	S	82	DOWN	80
5	S	64	S	20	UP	40 ^d
6	R	65	rac. ^e	70	DOWN	62

^a All reactions are carried out with commercially available racemic or *S*-benzoin.

^b Enantiomeric excess.

^c Using dihydropyridine and benzoin in a 1:1 ratio.

^d *S*-(1) is converted through autoxidoreduction to (2) (CO up) (At maximum 50%).

^e The yield of *meso*-diol is dependent on the ratio dihydropyridine:benzoin. With a ratio of 1:2 (*R*-(1): rac. benzoin) a 100% yield can be obtained.

Table 2.I reveals that *S*-benzoin and *R*-(1) react exclusively to give *meso*-1,2-diphenyl-1,2-ethanediol, whereas *S*-benzoin with *S*-(1) does not react (entries 2 and 3). Presumably the reactions of *R*-(1) with *S*-benzoin and *S*-(1) with *R*-benzoin will occur quickly, whereas the reactions of *S*-(1) and *R*-(1) with the *S*- and *R*-substrate, respectively, will be rather slow. Support for this conclusion comes from the results of entry 4 (table 2.I) in which the enantiomeric excess increases upon conversion of the dihydropyridine (1) into the pyridinium cation (2). No enantiomeric pure (2) (CO up) [1] is formed since a part of *S*-(1) (at maximum 50%) is converted through autoxidoreduction (= two molecules of (1) form a complex by which one is oxidized and one is reduced). The results of entry 5 also show the difference in reactivity; the small quantity of 1,2-diphenyl-1,2-ethanediol originates from the minor presence of *R*-(1).

The high optical yield of the axial chiral pyridinium perchlorate (2) obtained from *R*-(1) (entry 2), supports the intermediacy of a controlled transition state. By adopting a transition state in line with the proposed Mg²⁺ complex of methyl benzoylformate with (1) [1], in which the methoxycarbonyl group was located *syn* with respect to the amide function, the enantioselective reduction of benzoin can be explained. *R*-(1) should induce the *R*-configuration in the prochiral carbonyl group of the substrate and *S*-(1) the corresponding *S*-configuration. Reduction of *R*-benzoin by *S*-(1) leads, therefore, to

meso-1,2-diphenyl-1,2-ethanediol (figure 2.1). Similarly, *S*-benzoin and *R*-(1), also give rise to the *meso*-diol.

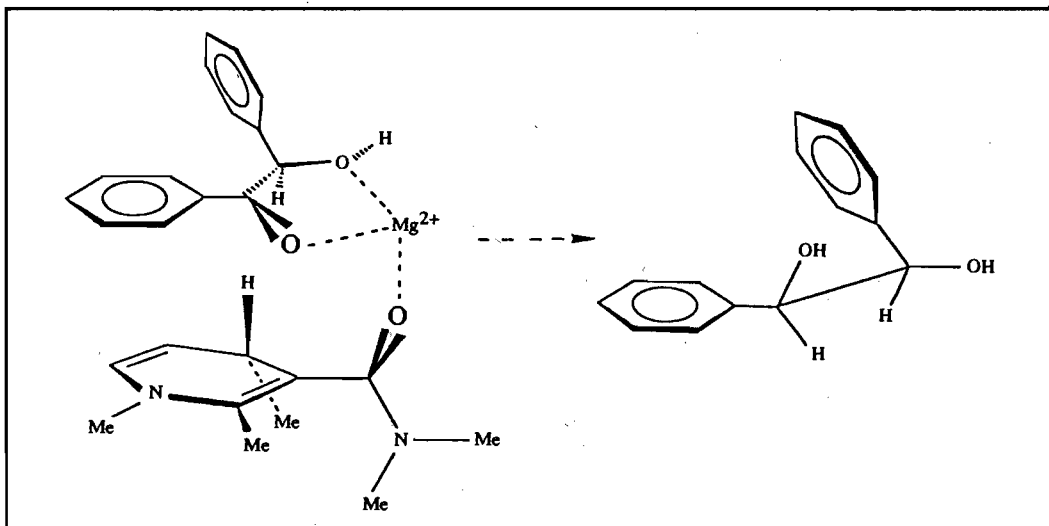


Figure 2.1 Schematic representation of the proposed ternary complex involved in the $\text{Mg}(\text{ClO}_4)_2$ -mediated hydride transfer from *S*-(1) to *R*-benzoin, leading to *meso*-1,2-diphenyl-1,2-ethanediol.

The formation of a chelate with the α -hydroxy group of benzoin on one hand and the presence of a relatively bulky phenyl group on the other hand may explain the high diastereoselectivity of the reduction. Upon formation of the Mg^{2+} complex, discrimination takes place between the two optical isomers of benzoin, i.e., *R*-(1) reacts with *S*-benzoin and not with *R*-benzoin; the opposite holds for *S*-(1). These results further prove that a ternary complex including chelation with the substrate is operative in $\text{Mg}(\text{ClO}_4)_2$ -induced NADH model reactions [1].

2.4 Conclusions

The reduction of benzoin (either optically active or racemic) by the NADH model compound (1) (either optically active or racemic) yields exclusively *meso*-1,2-diphenyl-1,2-ethanediol. This, together with the observed reluctance of *S*-(1) to react with *S*-benzoin, supports the intermediacy of a strictly organized transition state composed

of chelated substrate, dihydropyridine and magnesium ion. The remarkable selectivity of the dihydropyridines *R*-(1) and *S*-(1), towards *S*- and *R*-benzoin should, therefore, allow an efficient kinetic resolution of benzoin.

References

1. de Kok, P.M.T., Bastiaansen, L.A.M., van Lier, P.M., Vekermans, J.A.J.M. and Buck, H.M. *J. Org. Chem.* **54** (1989), 1313-1320.
2. Meyers, A.I. and Oppenlaender, T. *J. Am. Chem. Soc.* **108** (1986), 1989-1996.
3. Ohno, A., Yasuma, T., Nakamura, K. and Oka, S. *Israel J. Chem.* **28** (1987/88), 51-55.
4. Ohno, A., Yasuma, T., Nakamura, K. and Oka, S. *Bull. Chem. Soc. Jpn.* **59** (1986), 2905-2906.
5. Donkersloot, M.C.A. and Buck, H.M. *J. Am. Chem. Soc.* **103** (1981), 6554-6558.
6. de Kok, P.M.T., Donkersloot, M.C.A., van Lier, P.M., Meulendijks, G.H.W.M., Bastiaansen, L.A.M., van Hooff, H.J.G., Kanters, J.A. and Buck, H.M. *Tetrahedron* **42** (1986), 941-959.
7. Bastiaansen, L.A.M., Kanters, J.A., van der Steen, F.H., de Graaf, J.A.C. and Buck, H.M. *J. Chem. Soc., Chem. Commun.* (1986), 536-537.
8. Bastiaansen, L.A.M., Vermeulen, T.J.M., Buck, H.M., Smeets, W.J.J., Kanters, J.A. and Spek, A.L. *J. Chem. Soc., Chem. Commun.* (1988), 230-231.
9. van Hooff, H.J.G., van Lier, P.M., Bastiaansen, L.A.M. and Buck, H.M. *Recl. Trav. Chim. Pays-Bas* **101** (1982), 191-192.
10. Ohno, A., Ogawa, M. and Oka, S. *Tetrahedron Lett.* **29** (1988), 1951-1954.
11. Ohno, A., Kobayashi, H., Goto, T. and Oka, S. *Bull. Chem. Soc. Jpn.* **57** (1984), 1279-1282.
12. Ohno, A., Ohara, M. and Oka, S. *J. Am. Chem. Soc.* **108** (1986), 6438-6440.

CHAPTER 3*

MODELLING OF NAD⁺ AND NAD⁺ ANALOGUES IN HLADH USING MOLECULAR MECHANICS

Abstract

The interactions of NAD⁺ and some NAD⁺ analogues (modified only in their nicotinamide group) in a ternary complex with HLADH and DMSO were simulated using molecular mechanics calculations. Starting conformations were taken from X-ray crystallographic data reported by Eklund and co-workers [13]. In this study, NAD⁺ and its analogues were encaged by the constituent amino acids of the enzyme within a range of 6.0 Å from the NAD⁺/DMSO/Zn²⁺ complex.

Analysis of the calculational results show AMBER to be an useful tool for the evaluation of the essential NAD⁺-enzyme/DMSO/Zn²⁺ interactions. Moreover, it is able to provide structural information additional to the initially used X-ray crystallographic data and it is able to evaluate the essential interactions between NAD⁺ analogue, enzyme, DMSO and Zn²⁺ without the necessity of additional X-ray data.

A refinement of the AMBER model by the insertion of appropriate values for the "out-of-plane" rotation barrier proved to be reliable to describe the "out-of-plane" rotation as the calculated result for NAD⁺ ($\phi = 34^\circ$) was found to correlate closely with the available X-ray data ($\phi = 30^\circ$).

It is shown that the overall best fit of the energy-refined geometry of NAD⁺ with the initial X-ray geometry is obtained by fixing the adenine amino group at its initial positions, introducing specific values for the "out-of-plane" rotation barrier and using negatively charged deprotonated Cys 46 and Cys 174 residues.

* This chapter has been composed of parts from:

P.M.T. de Kok, N.A. Beijer, H.M. Buck, L.A.AE. Sluyterman and E.M. Meijer, *Recl. Trav. Chim. Pays-Bas* 107 (1988), 355-361.

P.M.T. de Kok, N.A. Beijer, H.M. Buck, L.A.AE. Sluyterman and E.M. Meijer, *Eur. J. Biochem.* 175 (1988), 581-585.

N.A. Beijer, H.M. Buck, L.A.AE. Sluyterman and E.M. Meijer, *Biochim. Biophys. Acta* 1039 (1990), 227-233.

3.1 Introduction

In order to obtain fundamental insight into the relationship between structure and function of NAD^+ and HLADH, we developed a molecular mechanics model in which both NAD^+ and NAD^+ analogues are analyzed in their interaction with the enzyme.

First we attempted, following the elegant work of Kollman [1-4], to simulate the interactions of HLADH and NAD^+ in a ternary complex with DMSO using the AMBER molecular mechanics program. In this study NAD^+ was encaged by a limited number of amino acids of the enzyme. It will be shown that the AMBER molecular mechanics method can give a reasonably good estimate of the coenzyme geometry in the active site of the complex.

The results with NAD^+ prompted us to apply the AMBER molecular modelling package to minimize the conformational energy of several NAD^+ analogues within the constructed cage of amino acids. Of special interest are those which are modified in the reactive part, the nicotinamide moiety (figure 3.1). For the corresponding HLADH/coenzyme complexes no X-ray data are available. Thus this study presents a novel approach to estimate ternary complex coenzyme geometries independent of the availability of additional X-ray data.

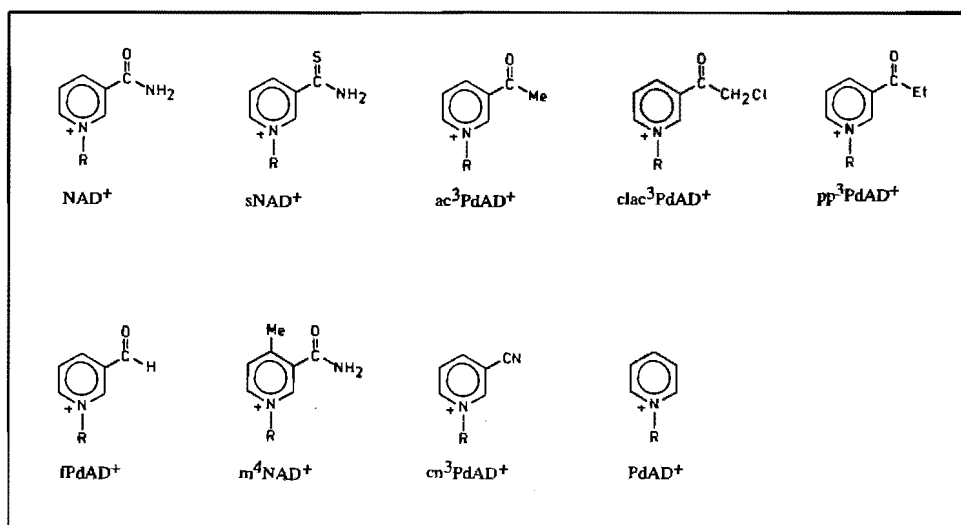


Figure 3.1 Structures of NAD^+ and NAD^+ analogues. Only the nicotinamide part is displayed.

In order to rationalize the activity of the coenzymes studied, two factors must be considered, (a) the position of the pyridinium ring and (b) the torsion angle between the carboxamide (or analogues thereof) side chain and the pyridinium ring (the "out-of-plane" rotation). However, for the determination of the carboxamide (or analogues) "out-of-plane" rotation, a refinement of the molecular mechanics model is necessary.

In this chapter we describe the procedure followed using the AMBER molecular modelling package. For details the reader is referred to the published papers [5-7].

3.2 The AMBER model

3.2.1 Introduction

We used the molecular mechanics program AMBER (version 3.0) [8] to build models of molecules and calculated their interactions using an empirical energy function. Molecular mechanics has the advantage that the minimum energy can be determined very rapidly for complex systems, something that is impossible with the more time-consuming quantum mechanical approaches. The energetically preferable conformation of NAD⁺ and NAD⁺ analogues, within the active site of an enzyme/substrate/Zn²⁺ complex, is obtained by minimizing the total energy function, which consists of separate terms covering bond-stretching (I), -bending (II) and torsional (III), as well as van der Waals, electrostatic (IV) and hydrogen bond (V) interactions (eqn. (3.1)).

$$\begin{aligned}
 E_{\text{total}} = & \sum_{\text{bonds}} K_R (R - R_{\text{eq}})^2 + \sum_{\text{angles}} K_\theta (\theta - \theta_{\text{eq}})^2 + \sum_{\text{dihedrals}} \frac{V_n}{2} [1 + \cos(n\phi - \gamma)] \\
 & \text{I} \qquad \qquad \qquad \text{II} \qquad \qquad \qquad \text{III} \\
 & + \sum_{i < j} \left(\frac{A_{ij}}{R_{ij}^{12}} - \frac{B_{ij}}{R_{ij}^6} + \frac{q_i q_j}{\epsilon R_{ij}} \right) + \sum_{\text{H bonds}} \left(\frac{C_{ij}}{R_{ij}^{12}} - \frac{D_{ij}}{R_{ij}^{10}} \right) \\
 & \qquad \qquad \qquad \text{IV} \qquad \qquad \qquad \qquad \qquad \qquad \qquad \qquad \qquad \text{V}
 \end{aligned} \tag{3.1}$$

Energy refinement and minimization using analytical gradients were performed until the root-mean-square (RMS) gradient of the energy was less than $0.1 \text{ kcal.}\text{\AA}^{-1}$. Additional semi-empirical parameters, which could not be obtained from the standard AMBER parameter set, are listed in appendix A. Standard bond lengths and bond angles were employed and harmonic force constants were either obtained directly from literature or extrapolated [9,10]. We used the MNDO semi-empirical molecular orbital method to calculate atomic charges. All groups, containing hydrogen atoms not essential for hydrogen bonding, are treated as united atoms, i.e., atomic charges of the hydrogen atoms are added to the charge of the adjacent atom to which they are bonded. All AMBER energy minimization procedures were performed using the distance-dependent dielectric constant $\epsilon = R_{ij}$, damping long-range interactions in favour of short-range polarization interactions. This is likely to be the best simulation of the distance dependency of the dielectric constant within proteins [10-12].

The calculations were performed on a VAX 11/785 computer. Examination of the resulting conformations was achieved using the ANAL module of AMBER in order to calculate the interaction energies, and Chem-X, an interactive computer graphics program (July 1987 update, copyright Chemical Design Oxford Ltd, Oxford), was used to generate stereodiagrams.

3.2.2 Starting geometries

AMBER calculations require starting geometries of the structures to be calculated. For this, we employed the X-ray crystallographic data for the ternary complex of HLADH/NAD⁺/DMSO (2.9 Å resolution, crystallographic R factor of 0.22) as reported by Eklund et al. [13], which were readily retrievable from the Brookhaven Protein Database.

3.2.2.1 Enzyme

Since AMBER can only perform its calculations with a limited number of atoms, the core of the enzyme has to be represented by a "cage" which is constructed of a relatively small number of amino acids, each fixed at its initial (X-ray) position. In order to obtain a "sealed" construction, 44 amino acids within a range of 6.0 Å from the coenzyme/Zn²⁺/DMSO complex, were selected. The residue numbers of the amino acids

involved are: 46-48, 51, 56, 57, 67, 68, 93, 94, 116, 140, 141, 173-175, 178, 182, 200-204, 222-225, 228, 268, 269, 271, 274, 291-295, 316-320, 362 and 369. Their full names are listed in appendix B. Enlargement of the cut-off distance did not result in any improvement of the results of the calculations. All parameters required could be obtained from the standard AMBER data base.

Conformational changes of the active site amino acids as a result of the rather small modifications of the nicotinamide moiety only, are neglected in our calculations. As far as we know, conformational changes in the enzyme due to modification of the pyridine moiety of the coenzyme have not been reported in literature [14].

3.2.2.2 Coenzyme

NAD⁺

Since AMBER does not have all parameters needed in its initial data base, we have introduced these parameters by creating additional data bases, which are listed in appendix A. Parameters for adenine, ribose and the phosphate groups were retrieved directly from the AMBER data base, whereas parameters used for the nicotinamide moiety were obtained from MNDO calculations (bond lengths, bond angles, torsion angles and charges) or estimated in accordance with data reported in literature (harmonic force constants) [9,10]. The geometry of NAD⁺ was taken from the X-ray data. Hydrogen atoms involved in hydrogen bonding were added with the computer graphics modelling program Chem-X (ribose OH's, nicotinamide NH's and adenine NH's).

NAD⁺ analogues

The three-dimensional structure of the NAD⁺ analogues were derived directly from the X-ray NAD⁺ geometry using Chem-X. Structural parameters not available in the AMBER data base were added [14] using standard bond-lengths and bond-angles (appendix A). Harmonic force constants were either obtained directly from literature or extrapolated [9,10]. Atomic charges were calculated using MNDO.

3.2.2.3 DMSO

The starting conformation was taken from the X-ray data. AMBER parameters were added to the AMBER data base (appendix A) and charges were calculated using MNDO.

3.2.2.4 Zinc

The formal charge of the zinc ion in the catalytic site of the ternary complex is introduced as plus two (see also discussion later on). AMBER parameters were estimated according to procedures reported in literature [9,10].

During the calculations, the zinc ion was fixed at its initial (X-ray) position.

3.2.3 Results and discussion

3.2.3.1 NAD⁺ geometry

The first case studied was the energy refinement of the NAD⁺ coenzyme molecule within the core of amino acids, employing the initial AMBER parameter set for all constituent amino acids of the "cage". Conformational restraints on the position of the coenzyme molecule were not included. In order to visualize the effects of energy minimization of the geometry of NAD⁺, both the initial NAD⁺ (X-ray) conformation as well as the energy-refined structure are depicted in figure 3.2. The initial NAD⁺ geometry may be somewhat erroneous owing to the limited resolution of the X-ray data. These inaccuracies are likely to be corrected systematically during the energy minimization procedures.

The torsion angles of the X-ray geometry of NAD⁺ and the conformation after energy refinement are included in table 3.I.

Figure 3.2 and table 3.I clearly show that energy refinement of the X-ray geometry of NAD⁺ induces some conformational changes. In addition to minor conformational changes observed in the nicotinamide mononucleoside moiety, the perturbation of the adenosine diphosphate unit, and in particular that of the phosphate bridge, is most pronounced.

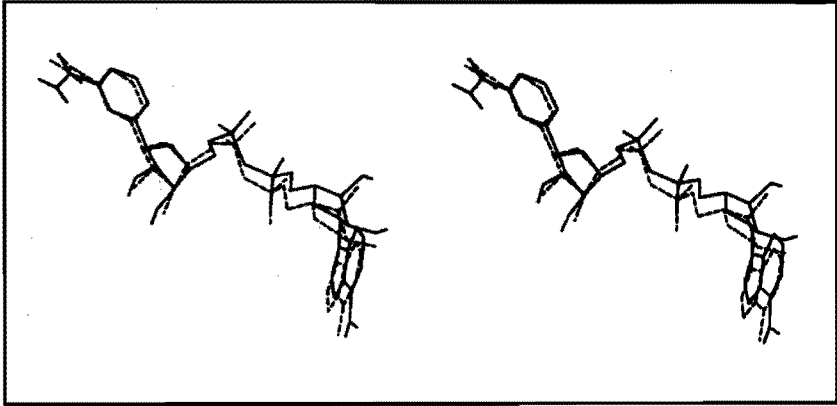


Figure 3.2 Stereodiagram of the energy-refined NAD⁺ geometry (—). The structure represented in broken line (-----) is the geometry of the NAD⁺ coenzyme molecule prior to energy refinement (X-ray). Neither the amino acids, nor the zinc ion are drawn since these atoms are not allowed to move during energy refinement.

Table 3.1 Conformational parameters (degrees) of NAD⁺ bound to HLADH with neutral and negatively charged cysteine 46 and 174 residues and to *Bacillus stearothermophilus* GAPDH [15]. Nomenclature of the coenzyme torsion angles is depicted in figure 3.3.

	χ_A	γ_A	β_A	α_A	ζ_N	ζ_N	α_N	β_N	γ_N	χ_N
HLADH X-ray	264	281	147	106	85	207	59	214	39	258
HLADH neutral cys	252	288	150	70	85	211	54	185	49	244
HLADH negative cys	253	291	153	65	90	204	60	175	61	252
GAPDH X-ray ^a	255- 258	286- 295	146- 157	73- 81	81- 88	197- 205	65- 80	162- 172	56- 67	76- 83 ^b

^a The range of variation of the torsion angles detected for the four subunits is presented by listing the minimal and maximal values, respectively.

^b Syn conformation of the nicotinamide group in NAD⁺ bound to GAPDH.

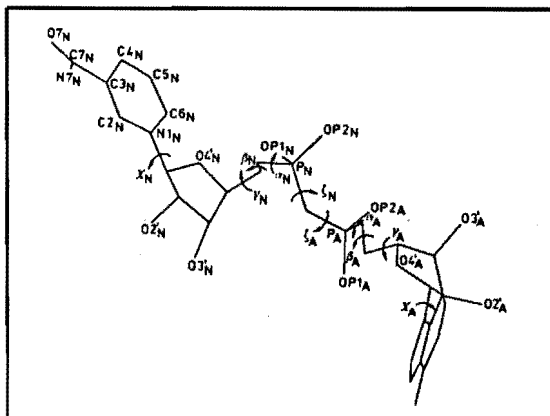


Figure 3.3 Nomenclature of the coenzyme torsion angles and the atoms used in the text (adopted from Eklund et al. [13], in accordance with the IUPAC-IUB convention of 1983).

However, one can easily expect the AMP repositioning to be the result of the displacement of the adenine moiety.

In order to test the validity of this assumption, we carried out energy refinement while restraining the exocyclic adenine amino group to its initial position. In this context it should be noted that enzymatic experiments show that immobilization of the coenzyme within the enzyme or on an inert support, using the adenine amino group, has no marked effect on its activity [16]. Figure 3.4 shows the energy-refined structures of restrained NAD⁺ relative to the initial NAD⁺ conformation.

In contrast to the situation depicted in figure 3.2, the most relevant discrepancies are

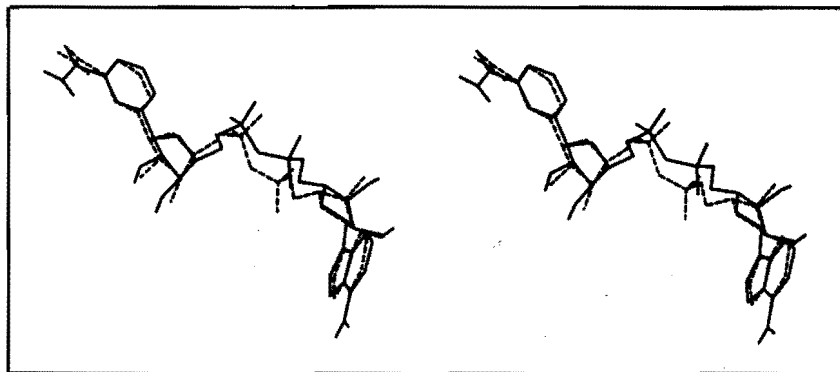


Figure 3.4 Conformations of NAD⁺ prior to (-----) and after (—) energy refinement with the adenine amino group fixed at its initial position.

in this case observed in the phosphate bridge.

The distance between the phosphate oxygen atom and the Lys 228 nitrogen atom in the X-ray structure is 5.7 Å. This distance, resulting in neglectable hydrogen bonding between Lys 228 and the AMP phosphate group, is large enough to accommodate a water molecule. This water molecule probably could not be detected owing to insufficient resolution of the X-ray analysis. Skarzynski and co-workers [15], on the other hand, showed in their high resolution crystallographic study of a binary complex of NAD^+ and GAPDH from *Bacillus stearothermophilus* (resolution of 1.8 Å, crystallographic R factor of 0.177) that several water molecules are included in the region of the phosphate bridge. In view of the fact that the coenzyme binding domains of GAPDH and HLADH show a close resemblance, resulting in similar binding conformations of NAD^+ (table 3.I), it is safe to assume that at least one water molecule is involved in hydrogen bonding with the phosphate bridge of NAD^+ in HLADH. In order to evaluate its effect, a single water molecule was introduced in the initial Eklund X-ray structure just between the adenosine phosphate group and the amino group of the Lys 228 side chain. The system obtained was submitted to energy refinement, restraining all atoms at their initial positions, except for those of the water molecule added. Subsequently, the entire structure, i.e., coenzyme, DMSO and the water molecule, was allowed to minimize energy while retaining restraints only on the position of the core of amino acids, the zinc ion and the adenosine amino group. Analysis of the final geometry revealed that the conformational change of the phosphate group was essentially reduced. (The shift of the AMP phosphor atom upon energy refinement is 0.7 Å instead of 1.3 Å found in absence of the water molecule). The results (figure 3.5) indicate that the position of the phosphate group is largely governed by H-bonding interactions in which at least one water molecule is involved.

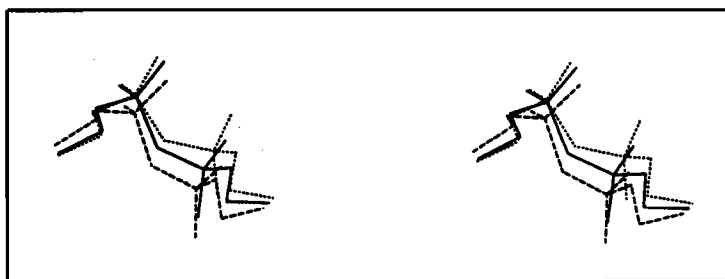


Figure 3.5 Region of the phosphate bridge of the initial NAD^+ geometry (-----), the energy-refined geometries without (.....) and with (—) an additional water molecule. The AMP phosphate group is situated at the right-hand side. The position of both ribose units is not affected significantly.

It can be expected that determination of the exact position of the water molecule (or molecules) may reduce the conformational changes even more. At any rate it should be noted that the conformation of the phosphate bridge does not affect the position of the nicotinamide moiety in the active site.

In the AMBER parameter set, parameters for the cysteine residues are available only for the neutral state. This means that some interactions between zinc and the core of amino acids are neglected. We introduced negatively charged cysteine residues via modification of the AMBER data base, i.e., AMBER parameters for the negatively charged cysteine residues were taken directly from the AMBER parameter set except for the atomic charges. The charges were derived from MNDO calculations of neutral cysteine adding one formal negative charge to the sulphur atoms. Figure 3.6 depicts the energy-refined NAD^+ geometry with the introduction of negatively charged cysteine residues and with the restraint on the position of the zinc ion. Torsion angles are given in table 3.I.

Figure 3.6, comparing the final geometries of NAD^+ using neutral and negatively charged cysteine, demonstrates the shift of the nicotinamide group towards Cys 174. The same effect expected for Cys 46 is however totally overshadowed by the enhanced repulsion between the sulphur atom of the cysteine residue and the nicotinamide-linked ribose oxygen atoms. This feature induces a perturbation of the position of the ribose unit at issue, increasing the distance between the sulphur atom and $\text{O2}'_N$ and $\text{O3}'_N$, respectively, simultaneously rotating $\text{O4}'_N$ towards the sulphur atom.

In addition, figure 3.6 clearly shows that the position of the nicotinamide group of the energy-refined geometry with negatively charged cysteine residues matches the Eklund X-ray NAD^+ geometry more precisely. In particular the C3_N and C5_N atoms of the X-ray and the energy-refined geometries are almost superimposable.

In conclusion, energy refinement of NAD^+ results in a geometry which is closely related to the actual structure of the NAD^+ determined with X-ray analysis. The overall best fit is observed by fixing the adenine amino group at its initial position, introducing a water molecule between the nicotinamide mononucleotide phosphate group and Lys 228, and using negatively charged deprotonated Cys 46 and Cys 174 residues.

Since the actual structure of the phosphate bridge has shown to be of minor importance to the conformation of the nicotinamide group (vide supra), the presumed inclusion of a water molecule near the phosphate bridge binding region can be ignored. The same holds for the adenosine part of the coenzyme which justifies the introduction of a positional restraint on the exocyclic adenine NH_2 group in order to reduce the computational time.

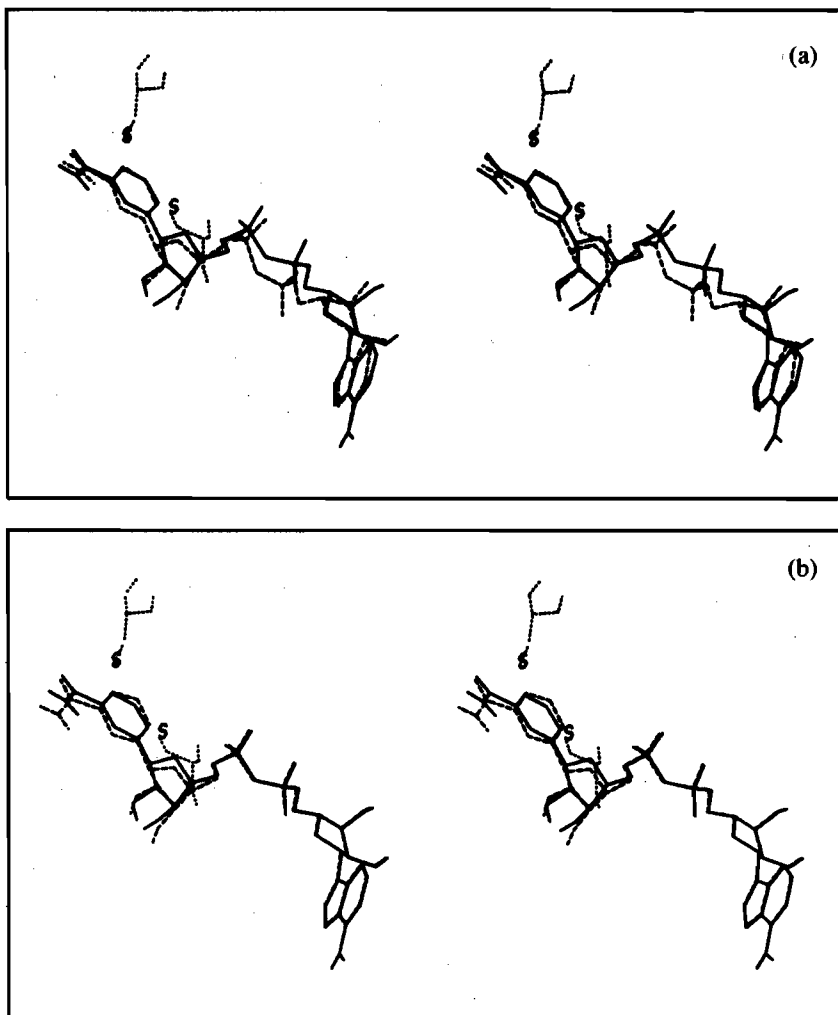


Figure 3.6 Energy-refined geometry of NAD^+ (—) bound to HLADH with negatively charged cysteine 46 and 174 (.....) residues, restraining the zinc ion and the adenine amino group at their initial positions. The structure represented by broken line (-----) is in figure (a) the initial NAD^+ geometry and in figure (b) the neutral cysteine energy-refined geometry of figure 3.4.

The results with NAD^+ prompted us to apply the AMBER molecular modelling package to simulate the conformation of several NAD^+ analogues in the active site of the ternary complex.

3.2.3.2 NAD⁺ analogue geometry

The simulation of the NAD⁺ analogue geometries are carried out by fixing the active site of HLADH constructed by a cage of 44 amino acids, the zinc ion and the exocyclic adenine NH₂ group at their initial positions. The cysteine residues of the core of amino acids (Cys 46 and 174) were introduced as negatively charged residues.

It should be noted that systematic errors in the energy-refined geometries of NAD⁺ and its analogues can occur in the minimization procedure. Since such deviations of the core of amino acids are systematically present in all minimization procedures, effects tend to cancel when two energy-refined structures are compared. From this it is evident that in order to evaluate the effect of substituents upon the NAD⁺ geometry, the energy-refined NAD⁺ geometry should be used as a reference.

Computer generated stereodiagrams (Chem-X) of the nicotinamide moiety of the optimized geometries, relative to the energy-refined geometry of the active part of NAD⁺ itself, are presented in figure 3.7. Since conformational discrepancies are restricted to the nicotinamide moiety only these regions of the NAD⁺ structures are drawn. Neither the zinc ion nor the amino acids are depicted since they are invariant during all calculations.

Table 3.II lists the numerical values of the torsion angles of the coenzyme analogues.

Table 3.II Conformational parameters (degrees) of energy-refined NAD⁺ and NAD⁺ derivatives. See figure 3.3 for nomenclature.

Compound	χ_A	γ_A	β_A	α_A	ρ_A	ρ_N	α_N	β_N	γ_N	χ_N
NAD ⁺	252	288	150	70	85	211	54	185	49	244
sNAD ⁺	250	287	151	70	82	215	52	186	52	246
ac ³ PdAD ⁺	252	287	150	71	84	213	55	185	55	264
clac ³ PdAD ⁺	252	287	150	70	84	212	55	184	55	267
pp ³ PdAD ⁺	251	288	150	70	84	212	54	184	55	267
PdAD ⁺	251	287	150	70	83	214	52	188	45	217
m ⁴ NAD ⁺	250	292	160	72	85	207	53	194	49	245
cn ³ PdAD ⁺	251	290	153	65	85	213	48	188	51	235

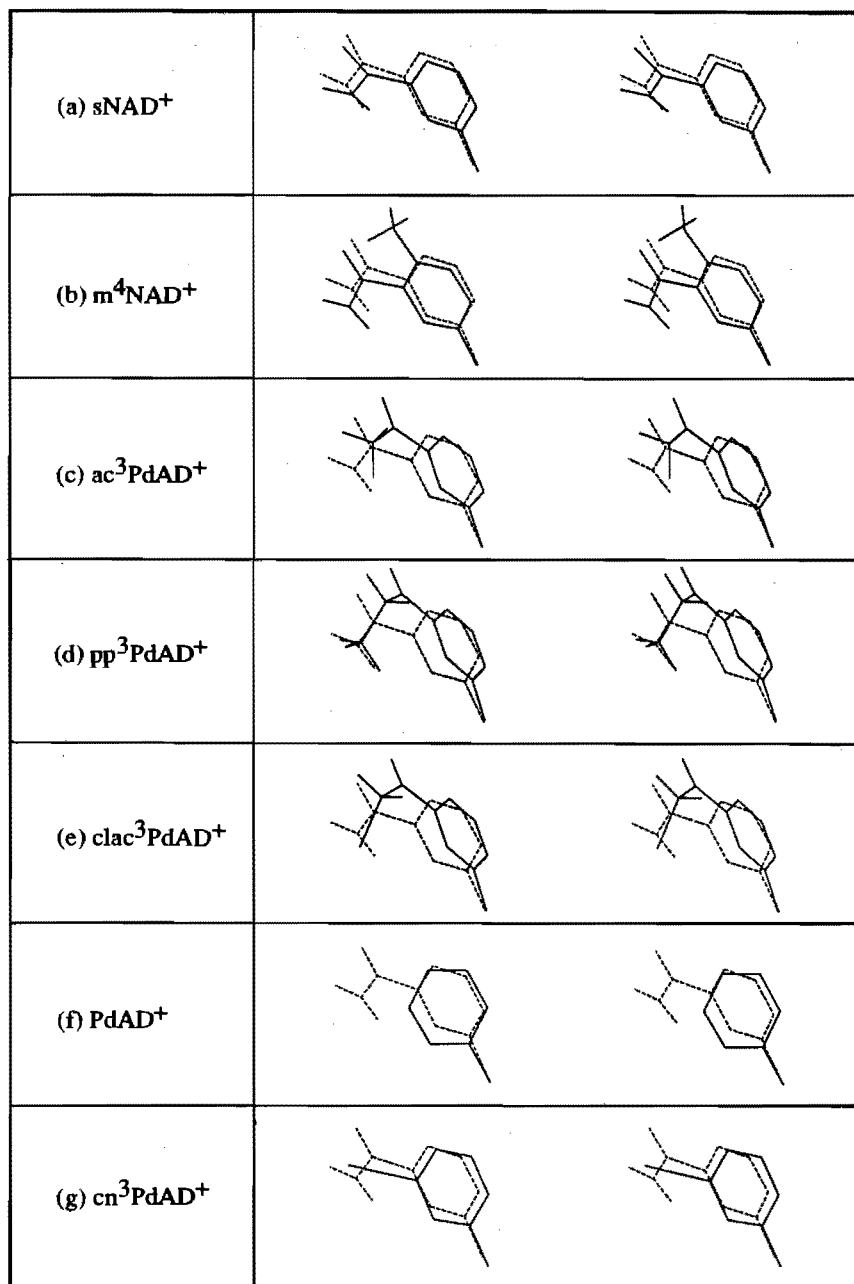


Figure 3.7 Stereodiagrams of the nicotinamide moiety of the optimized NAD⁺ analogue geometries (—). The structure represented by the broken line (-----) is the energy-refined geometry of the NAD⁺ coenzyme.

On the basis of energy-refined geometries, NAD⁺ and its analogues can be divided into three groups (table 3.III). Each group consists of derivatives with structures which are perturbed from the energy-refined NAD⁺ geometry in quite a similar manner (figure 3.7). The torsion angle of the glycosidic bond can serve as a probe for the description of the conformational changes of the pyridine moieties. This can be done because the ribose unit is hardly displaced upon energy refinement, and bond-distances and -angles of the nicotinamide moiety remain near to their optimal values.

At this stage we examined the availability of literature data concerning the kinetics of HLADH catalyzed reactions with NAD⁺ derivatives modified in the nicotinamide group. As far as we are aware, there are no detailed kinetic data available concerning HLADH. There are, however, overall kinetic data for lactate dehydrogenase (LDH) [17], an enzyme which has a coenzyme binding domain that is almost identical to that of HLADH. Although there is some ambiguity in applying calculations for HLADH to LDH, there is a qualitative consistency between the calculated conformation of the coenzyme analogues and their overall activity with LDH (table 3.III).

Table 3.III NAD⁺ and its analogues divided into three categories using the torsion angle (χ_N) and some overall activities of NAD⁺ analogues with LDH obtained from literature [17].

Category	Analogue	χ_N (degrees)	V_{max} (rel, %)
I	NAD ⁺	244.4	100 ^a
	sNAD ⁺	245.0	26-74 ^a
	m ⁴ NAD ⁺	246.2	-
II	ac ³ PdAD ⁺	263.7	4-33 ^a
	clac ³ PdAD ⁺	267.0	5 ^b
	pp ³ PdAD ⁺	267.2	3- 6 ^a
III	PdAD ⁺	217.2	-
	cn ³ PdAD ⁺	234.5	-

^a Range covering values for Dogfish, Rabbit and Beef LDH.

^b Dogfish LDH.

Proceeding from category I to II the torsion angle of the glycosidic bond increases considerably. These effects are certainly due to the absence in analogues of category II of the nicotinamide amino group. The size of the pyridine moieties of the analogues of category III, on the other hand, is smaller than the size of categories I and II. This feature, in combination with the total absence of the amide group and its interactions renders the pyridine moiety rather mobile.

NAD^+ and sNAD^+ , both category I, are fully active. Compounds of category II are also active, though to a smaller extent. Those of category III, deviating most from NAD^+ conformation, exhibit no activity. Nevertheless they are competitive inhibitors with respect to NAD^+ , implying that they bind to the same enzyme site.

m^4NAD^+ is a special case: it is a strong competitive inhibitor because it binds to HLADH in the same way as NAD^+ does. The 4-methyl group, owing to its electron releasing capacity however, renders the redox potential too negative for coenzyme activity [18].

In conclusion, the results presented above demonstrate AMBER to be an useful tool for evaluating the essential interactions governing the geometry of NAD^+ and NAD^+ analogues in the active site of the ternary complex of HLADH/ NAD^+ /DMSO. Furthermore, the method seemed to be capable at first sight, to correlate the geometry (pyridinium position) of the NAD^+ analogues within the ternary complex as calculated by AMBER with their reactivity in enzymatic redox reactions.

However, a further refinement of the AMBER model seems necessary for more accurate determination of the geometries of the coenzymes (e.g., the "out-of-plane" rotation of the carboxamide group (or analogues)).

3.3 Refinement of the AMBER model describing the "out-of-plane" orientation

3.3.1 Introduction

In this section a refinement of the AMBER model is described in which special attention is paid to the "out-of-plane" torsion of the carboxamide group (or analogues, figure 3.8) to elucidate the exact orientation of the carboxamide group. The "out-of-plane" orientation has been shown to enhance greatly the rate of hydride transfer, bringing about stereoselectivity in nonenzymatic model systems related to the redoxcouple NAD^+/NADH [18-20].

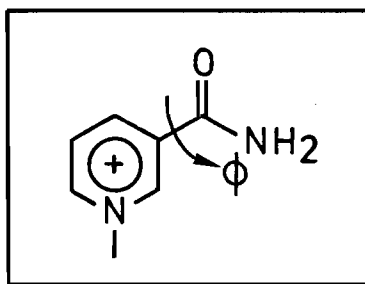


Figure 3.8 "Out-of-plane" rotation of the carboxamide side chain, $\phi = 0$: the CO group is situated in the plane of the pyridinium ring (in the orientation drawn).

3.3.2 Parameters for the "out-of-plane" orientation

The same overall procedure has been followed as described above, i.e., during the energy minimizations the amino acids, the zinc ion and the adenine amino group were fixed at their initial positions. The cysteine residues of the core of amino acids were introduced as negatively charged residues. Most harmonic force constants were obtained directly from the literature or extrapolated [9,10].

For the calculation of the "out-of-plane" rotation appropriate values for the rotation barriers V_n had to be inserted in the AMBER total energy function (eqn. (3.1)). However, for the pyridinium compounds no experimental values were found in literature and moreover quantum chemical calculations did not provide sufficiently reliable results [21,22]. The experimental values of the closely related benzene derivatives, benzamide, benzaldehyde and benzophenone [23,24] were therefore taken. These values may be assumed to be a close approximation to those of the pyridinium compounds NAD^+ (sNAD^+), fPdAD^+ and ac^3PdAD^+ , respectively, as benzaldehyde has the same rotation barrier as pyridine-3-aldehyde, 4.7 and 4.6 kcal.mol⁻¹, respectively [24]. The rotation barrier was neglected for NAD^+ and sNAD^+ , since for benzamide a mean "out-of-plane" rotation of $39^\circ \pm 2^\circ$ has been determined [25], i.e., very close to the 45° observed in the absence of any rotational barrier. (The difference in the introduced rotation barrier between the aldehyde and the ketone on the one hand and the amide on the other hand can be easily understood. The carboxamide group has its own resonance stabilization and therefore has no tendency for resonance interaction with the aromatic ring, whereas the aldehyde and ketone groups will do so. Their interactions will stabilize the flat conform-

ation and increase the barrier.)

The torsion potentials introduced for the coenzymes are summarized in table 3.IV.

Table 3.IV Parameters for the "out-of-plane" torsion angle of NAD^+ and its analogues.

Compound	$V_n/2$ (kcal.mol ⁻¹)	ϕ (degrees)	n
NAD^+	0.0	180	2
s NAD^+	0.0	180	2
ac ³ PdAD ⁺	1.55	180	2
fPdAD ⁺	2.35	180	2

3.3.3 Results and discussion

The described procedure of refinement proved to be reliable for NAD^+ as the calculational "out-of-plane" torsion angle of NAD^+ (34°) fits well with the X-ray value (30°) reported by Eklund et al. [13] (table 3.V).

The geometries of the energy-minimized s NAD^+ , ac³PdAD⁺ and fPdAD⁺, with

Table 3.V Conformational parameters (degrees) of energy-refined NAD^+ and NAD^+ derivatives. Nomenclature of the coenzyme (analogue) torsion angles is depicted in figures 3.3 and 3.8.

Compound	χ_A	γ_A	β_A	α_A	ζ_A	ζ_N	α_N	β_N	γ_N	χ_N	ϕ
NAD^+	253	292	153	65	91	201	57	185	53	271	34 (30 ^a)
s NAD^+	253	292	154	64	90	202	56	187	55	270	47
ac ³ PdAD ⁺	253	292	153	65	90	201	57	185	55	272	6.5
fPdAD ⁺	253	292	153	65	90	203	56	191	50	274	9

^a Value obtained from X-ray analysis [13].

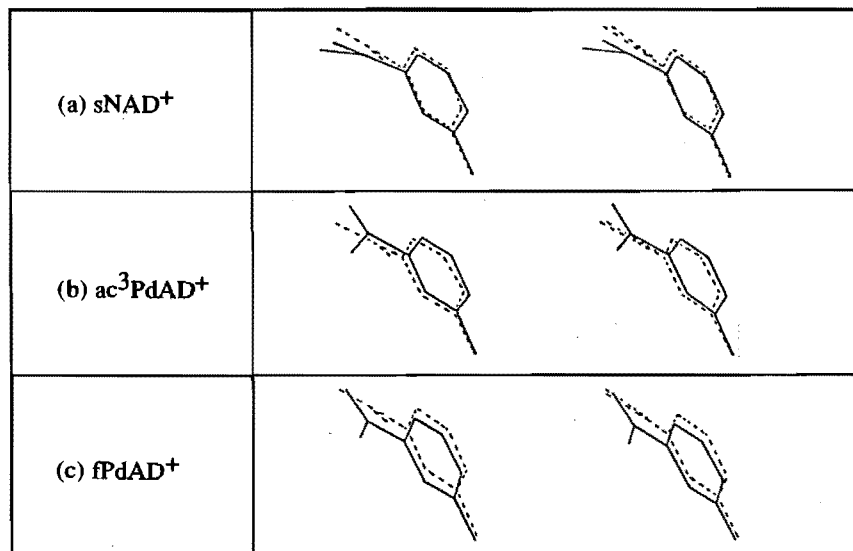


Figure 3.9 Stereodiagrams of the nicotinamide moiety of the optimized NAD⁺ analogue geometries (—). The structure represented by the broken line is the energy-refined geometry of NAD⁺.

respect to the energy-refined NAD⁺ geometry, are given in figure 3.9. Since conformational differences (table 3.V) are restricted to the nicotinamide (or analogues) moiety, only these regions of the structures are drawn. Neither the zinc ion, nor the amino acids are depicted since they are invariant during all calculations.

As far as the "out-of-plane" torsion angle is concerned the thiocarbonyl group of the energy-refined sNAD⁺ structure shows a larger torsion angle (47°) than the carbonyl group of NAD⁺ (table 3.V), while the torsion angles of ac³PdAD⁺ and fPdAD⁺ are strongly diminished (6.5° and 9°, respectively).

Figure 3.9 shows that in contrast to sNAD⁺ the position of the pyridinium rings of ac³PdAD⁺, cn³PdAD⁺ and fPdAD⁺ deviate from the NAD⁺ pyridinium ring. It can also be observed that fPdAD⁺ exhibits an opposite deviation compared to ac³PdAD⁺ and cn³PdAD⁺.

In conclusion, with the refinement of the presented AMBER model we are now able to determine more precisely the exact geometry of the NAD⁺ analogues. In the next chapter we will correlate the enzymatic activity of NAD⁺ and its analogues with HLADH

on the basis of their conformation (pyridinium position and "out-of-plane" rotation) in the active site as determined with AMBER molecular mechanics.

3.4 Conclusions

The results presented above establish AMBER as an useful tool for evaluating the essential interactions governing the geometry of NAD^+ in the active site of the ternary complex of HLADH/ NAD^+ /DMSO.

The overall best fit is observed by fixing the amino acids, the zinc ion and the adenine amino group at their initial positions, using negatively charged deprotonated Cys 46 and 174, and introducing specific rotation barriers for the "out-of-plane" rotation. With the introduction of specific rotation barriers as a refinement of the AMBER model we are able to determine exact geometries of NAD^+ analogues. The calculated "out-of-plane" torsion angle (ϕ) of NAD^+ (34°) fits well with the X-ray value (30°).

Furthermore there are strong indications that this calculational method can even provide information additional to data obtained from X-ray crystallographic studies. For example, we have shown that the inclusion of a water molecule near the phosphate bridge of NAD^+ leads to a better fit with the Eklund model.

It can also be concluded that conformational changes of the phosphate bridge and the AMP subunit do not affect the geometry of the nicotinamide group. This finding is in accordance with observations of Sicsic and co-workers [26,27], who showed that several fragments of $\text{NAD}^+(\text{H})$, nicotinamide mononucleotide and -mononucleoside (in the presence of AMP), are functional in enzyme-catalyzed redox reactions. In addition, immobilization using the exocyclic amino group of adenine does not interfere with the activity of NAD^+ .

In view of all these considerations, AMBER would appear to be capable of giving a reasonably accurate description of the geometry of NAD^+ (and analogues) bound in the active site of an enzyme.

References

1. Blaney, J.M., Weiner, P.K., Dearing, A., Kollman, P.A., Jorgensen, E.C., Oatley, S.J., Burridge, J.M. and Blake, C.C.F. *J. Am. Chem. Soc.* **104** (1982), 6424-6434.

2. Wipff, G., Dearing, A., Weiner, P.K., Blaney, J.M. and Kollman, P.A. *J. Am. Chem. Soc.* 105 (1983), 997-1005.
3. Oatley, S.J., Blaney, J.M., Langridge, R. and Kollman, P.A. *Biopolymers* 23 (1984), 2931-2941.
4. Tilton, R.F., Singh, U.C., Weiner, S.J., Connolly, M.L., Kuntz, I.D., Kollman, P.A., Max, N. and Case, D.A. *J. Mol. Biol.* 192 (1986), 443-456.
5. de Kok, P.M.T., Beijer, N.A., Buck, H.M., Sluyterman, L.A.AE. and Meijer, E.M. *Recl. Trav. Chim. Pays-Bas* 107 (1988), 355-361.
6. de Kok, P.M.T., Beijer, N.A., Buck, H.M., Sluyterman, L.A.AE. and Meijer, E.M. *Eur. J. Biochem.* 175 (1988), 581-585.
7. Beijer, N.A., Buck, H.M., Sluyterman, L.A.AE. and Meijer, E.M. *Biochim. Biophys. Acta* 1039 (1990), 227-233.
8. Weiner, P.K. and Kollman, P.A. *J. Comp. Chem.* 2 (1981), 287-303.
9. Weiner, S.J., Kollman, P.A., Case, D.A., Singh, U.C., Ghio, C., Alagona, G., Profeta, S. and Weiner, P.K. *J. Am. Chem. Soc.* 106 (1984), 765-784.
10. Weiner, S.J., Kollman, P.A., Nguyen, D.T. and Case, D.A. *J. Comp. Chem.* 7 (1986), 230-252.
11. Warshel, A. *J. Phys. Chem.* 83 (1979), 1640-1652.
12. Rees, D.C. *J. Mol. Biol.* 141 (1980), 323-326.
13. Eklund, H., Samama, J.P. and Jones, T.A. *Biochemistry* 23 (1984), 5982-5996.
14. Biellmann, J.F. *Acc. Chem. Res.* 19 (1986), 321-328.
15. Skarzynski, T., Moody, P.C.E. and Wonacott, A.J. *J. Mol. Biol.* 193 (1987), 171-187.
16. Mosbach, K. in "Enzymes in Organic Synthesis, Ciba Foundation Symposium 111" (R. Porter and S. Clark, eds.), Pitman, London, (1985), 57 and references cited therein.
17. Samama, J.P., Marchal-Rosenheimer N., Biellmann, J.F. and Rossmann, M.G. *Eur. J. Biochem.* 120 (1981), 563-569.
18. de Kok, P.M.T., Donkersloot, M.C.A., van Lier, P.M., Meulendijks, G.H.W.M., Bastiaansen, L.A.M., van Hooff, H.J.G., Kanters, J.A. and Buck, H.M. *Tetrahedron* 42 (1986), 941-959.
19. Beijer, N.A., Vekemans, J.A.J.M. and Buck, H.M. *Recl. Trav. Chim. Pays-Bas* 109 (1990), 434-436.
20. de Kok, P.M.T., Bastiaansen, L.A.M., van Lier, P.M., Vekemans, J.A.J.M. and Buck, H.M. *J. Org. Chem.* 54 (1989), 1313-1320.
21. Donkersloot, M.C.A. and Buck, H.M. *J. Am. Chem. Soc.* 103 (1981), 6554-6558.

22. Cummins, P.L. and Gready, J.E. *J. Mol. Struct. (Theochem)* **183** (1989), 161-174
23. Kakar, R.K., Rinehart, E.A., Quade, C.R. and Kojima, T. *J. Chem. Phys.* **52** (1970), 3803-3813.
24. Miller, F.A., Fateley, W.G. and Witkowski, R.E. *Spectrochim. Acta A* **23** (1967), 891-908.
25. Pierens, R.K. and Williams, A.J. *J. Chem. Soc. Perkins Trans. II*, (1980), 235-242.
26. Sicsic, S., Durand, P., Langrené, S. and Le Goffic, F. *FEBS Lett.* **176** (1984), 321-324.
27. Sicsic, S., Durand, P., Langrené, S. and Le Goffic, F. *Eur. J. Biochem.* **155** (1986), 403-407.

CHAPTER 4*

RELATIONSHIP BETWEEN REACTIVITY AND SIMULATED CONFORMATION OF NAD⁺ AND NAD⁺ ANALOGUES

Abstract

In the present chapter we show that the enzymatic activity of NAD⁺ and its analogues (C(O)NH₂ replaced by C(S)NH₂, C(O)CH₃, C(O)H and CN) with HLADH can be rationalized by their conformation in the active site determined with AMBER molecular mechanics. In order to establish the relation between the hydride transfer rate and the conformation of the NAD⁺ and its analogues, kinetic experiments with the poor substrate isopropanol were carried out.

It appears that the enzymatic activity can be readily explained by the geometry of the pyridinium ring, in particular the magnitude of the "out-of-plane" rotation of the carboxamide side chain (or analogues). The latter is nicely illustrated in the case of cn^3PdAD^+ which lacks any "out-of-plane" rotation and concomitantly exhibits no significant enzymatic activity.

* This chapter has been composed of parts from:

N.A. Beijer, H.M. Buck, L.A.AE. Sluyterman and E.M. Meijer, *Biochim. Biophys. Acta* 1039 (1990), 227-233.

N.A. Beijer, H.M. Buck, L.A.AE. Sluyterman and E.M. Meijer, *Ann. N. Y. Acad. Sci.* (1990), in press.

4.1 Introduction

As already mentioned before, more insight into the mechanism of dehydrogenase action can be gained by examining the effects of replacing NAD^+ by NAD^+ analogues. Of special interest are those that are modified in the reactive part, the nicotinamide moiety. Kinetic data with such analogues have been published for various dehydrogenases [1-11], but no systematic explanation has so far been provided for their reactivities. In the present chapter a qualitative explanation using molecular mechanics calculations is reported.

The chemical step in the enzymatic conversion is the hydride ion transfer from the alcohol to the coenzyme or vice versa. If NAD^+ is used as coenzyme and ethanol as substrate, the rate limiting step is the dissociation of the coenzyme from the enzyme [12]. On the other hand, when the poor substrate isopropanol is used, it has been shown by presteady-state measurements that the hydride transfer is rate-limiting [12]. In order to relate the hydride transfer rate to the conformation of the NAD^+ analogues in the active site, kinetic experiments with isopropanol were therefore carried out in this study. It is self-evident, that, for comparing various analogues, the intrinsic reactivity of each, i.e., the non-enzymatic reaction rate with dithionite, has also to be taken into account.

With reference to the required structural data, both the position of the pyridinium moiety relative to the substrate and the "out-of-plane" rotation ϕ of the side chain of the pyridinium ring should be studied.

In dehydrogenases the A- and B-specificity is determined by the spatial relationship of substrate and pyridinium moiety (A-specificity in HLADH, B-specificity in GAPDH). The "out-of-plane" rotation will therefore affect, not the specificity, but the rate of hydride transfer; for effective enzyme action the side chain carbonyl group should therefore be directed more or less towards the substrate. Such is indeed the case in HLADH ($\phi = 30^\circ$, [13]) and in GAPDH ($\phi = 22^\circ$, [14]) as observed by X-ray analysis.

For the present study we used the analogues $s\text{NAD}^+$, $ac^3\text{PdAD}^+$, $f\text{PdAD}^+$ and $cn^3\text{PdAD}^+$ carrying the pyridine side chains C(S)NH_2 , C(O)CH_3 , C(O)H and CN , respectively. For the corresponding HLADH/coenzyme complexes no X-ray data are available. We therefore resorted to molecular mechanics calculations to assess the geometry of the analogues and interactions with the enzyme.

It will be shown in the present chapter that the enzymatic activity of the NAD^+ and its analogues can be rationalized in terms of geometric features, taking into account the intrinsic reactivities.

4.2 Materials and methods

4.2.1 Enzyme kinetics

HLADH was purchased from Boehringer Mannheim. NAD^+ , ac^3PdAD^+ , sNAD^+ and fPdAD^+ were obtained from Sigma Chemical Company. The substrates ethanol and isopropanol, and the phosphates of the 0.047 M phosphate buffer used (with 0.25 mM EDTA, pH = 7.0, $\Gamma = 0.1$) were from Merck. The purity of the alcohols was checked using gas chromatography. Enzyme solutions were centrifuged prior to use. Kinetic experiments were carried out at 22°C on a Hitachi 150-20 UV/VIS spectrophotometer equipped with a data processor. The steady-state initial-rates of NAD^+ , sNAD^+ , fPdAD^+ and ac^3PdAD^+ , respectively, were measured following the formation of the reduced pyridine nucleotide at an appropriate wavelength (NAD^+/NADH : $\lambda = 340$ nm, $\epsilon = 6220$ $\text{M}^{-1}\text{cm}^{-1}$; $\text{sNAD}^+/\text{sNADH}$: $\lambda = 396$ nm, $\epsilon = 10000$ $\text{M}^{-1}\text{cm}^{-1}$; $\text{ac}^3\text{PdAD}^+/\text{ac}^3\text{PdADH}$: $\lambda = 363$ nm, $\epsilon = 9000$ $\text{M}^{-1}\text{cm}^{-1}$; $\text{fPdAD}^+/\text{fPdADH}$: $\lambda = 358$ nm, $\epsilon = 7800$ $\text{M}^{-1}\text{cm}^{-1}$ [8,15,16]). The concentration range of the coenzyme was 10-100 μM (with the exception of fPdAD^+ , which varied from 100 to 1000 μM). The substrate concentration ranged from 2 to 19 mM.

Kinetic parameters in the initial-rate equation [12]:

$$1/V = e/k_{\text{cat}} (1 + K_a/[A] + K_b/[B] + K_c/[A][B]) \quad (4.1)$$

were obtained from the primary and secondary plots of the initial-rate data. In eqn. (4.1), e is the concentration of enzyme active centres (twice the molar concentration); A and B represent coenzyme and substrate, respectively; K_a , K_b and K_c denote the kinetic coefficients.

At saturated ethanol concentration the measured k_{cat} values (data not shown) are in accordance with literature data [6,7,9-11,17,18].

4.2.2 Procedure for calculational studies

Energy calculations and total energy minimization energies were performed with the

AMBER molecular mechanics package (version 3.0) [19] on a VAX 11/785 computer.

The procedure is described in the previous chapter. The active site of HLADH was constructed from X-ray crystallographic data of a ternary complex of HLADH/NAD⁺/DMSO reported by Eklund and co-workers (2.9 Å resolution, crystallographic R factor of 0.22) [13] which was readily retrievable from the Brookhaven Protein Database. The three-dimensional structures of the NAD⁺ analogues were derived directly from the X-ray NAD⁺ geometry using an Chem-X (January 1989 update, copyright Chemical Design Oxford, Ltd Oxford). During the energy minimization the amino acids and the zinc ion were fixed at their initial positions. The cysteine residues of the core of amino acids (Cys 46 and 174) were introduced as negatively charged residues as described previously. All minimizations were performed until the RMS gradient value of the energy was less than 0.1 kcal.Å⁻¹, using the distance-dependent dielectric constant and treating all CH, CH₂ and CH₃ groups as united atoms.

Atomic charges were calculated using the MNDO semi-empirical molecular orbital method. Most harmonic force constants were obtained directly from the literature or extrapolated [20,21]. The dihedral torsion angle barrier for the carboxamide "out-of-plane" rotation was chosen as described in the previous chapter.

4.3 Results and discussion

4.3.1 Molecular mechanics calculations

The geometries of the energy-minimized sNAD⁺, ac³PdAD⁺, fPdAD⁺ and cn³PdAD⁺, with respect to the energy-refined NAD⁺ geometry, are given in figure 4.1 (equal to figure 3.9, except for cn³PdAD⁺). Since conformational differences (table 4.I) are restricted to the nicotinamide (or analogues) moiety, only these regions of the structures are drawn. Neither the zinc ion nor the amino acids are depicted since they are invariant during all calculations.

Figure 4.1 shows that in contrast to sNAD⁺ the position of the pyridinium rings of ac³PdAD⁺, cn³PdAD⁺ and fPdAD⁺ deviate from the NAD⁺ pyridinium ring. It can also be observed that fPdAD⁺ exhibits an opposite deviation compared to ac³PdAD⁺ and cn³PdAD⁺.

As far as the "out-of-plane" torsion angle is concerned the thiocarbonyl group of the

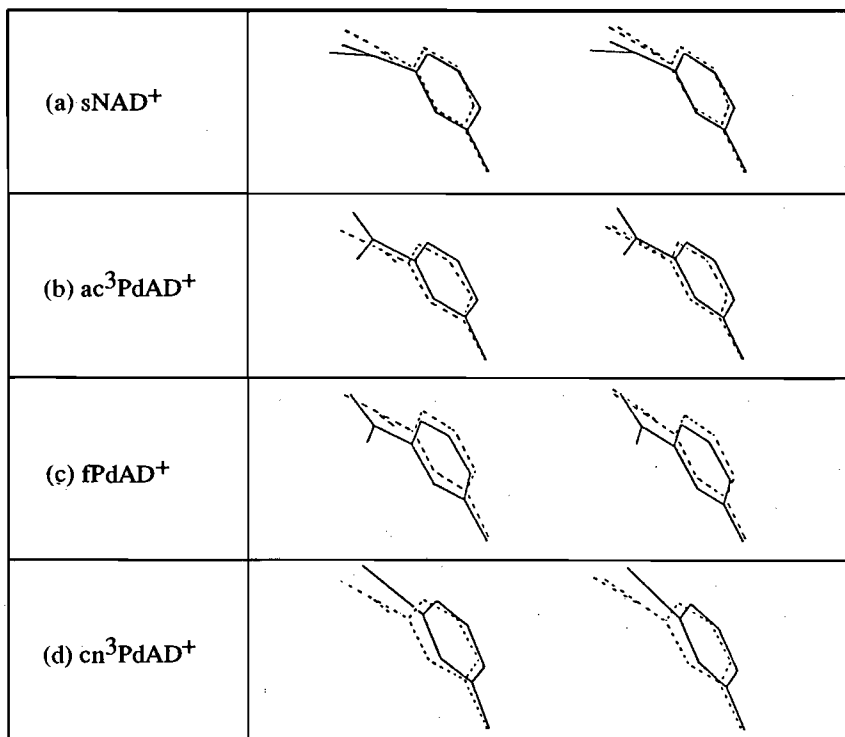


Figure 4.1 Stereodiagrams of the nicotinamide moiety of the optimized NAD⁺ analogue geometries (—). The structure represented by the broken line is the energy-refined geometry of NAD⁺.

Table 4.1 Conformational parameters (degrees) of energy-refined NAD⁺ and NAD⁺ derivatives (equal to table 3.V, except for cn³PdAD⁺).

Compound	χ_A	γ_A	β_A	α_A	ζ_A	ζ_N	α_N	β_N	γ_N	χ_N	ϕ
NAD ⁺	253	292	153	65	91	201	57	185	53	271	34
sNAD ⁺	253	292	154	64	90	202	56	187	55	270	47
ac ³ PdAD ⁺	253	292	153	65	90	201	57	185	55	272	6.5
fPdAD ⁺	253	292	153	65	90	203	56	191	50	274	9
cn ³ PdAD ⁺	253	291	153	65	91	201	57	186	55	272	-

energy-minimized sNAD⁺ structure shows a larger torsion angle (47°) than the carbonyl group of NAD⁺ (table 4.I), whereas the torsion angles of ac³PdAD⁺ and fPdAD⁺ are strongly diminished (6.5° and 9°, respectively). Obviously, cn³PdAD⁺ exhibits no "out-of-plane" rotation at all.

All this is further illustrated in figure 4.2, which outlines the position of the nicotinamide (or analogue) moiety of the coenzyme with respect to the main chain NH group of Phe 319 and the substrate DMSO. Relevant data are given in table 4.II. Particularly the long distance between the carbonyl oxygen of fPdAD⁺ and the sulphur atom of DMSO is noteworthy, as will be discussed later.

Table 4.II Geometric and kinetic data of energy-refined NAD⁺ and NAD⁺ derivatives.

Compound	ϕ (deg)	N(Phe 319)- O(C(O)R) (Å)	S(DMSO)- O(C(O)R) (Å)	C4(analog)- C4(NAD ⁺) ^a (Å)	k_{cat} ^b (rel)
NAD ⁺	34(30 ^c)	2.9 ± 0.2	4.2 ± 0.2		1
sNAD ⁺	47	3.4 ^d	3.9 ^d	0.2	4.12
ac ³ PdAD ⁺	6.5	2.9	4.4	0.4	2.35
fPdAD ⁺	9	2.9	5.1	0.6	0.12
cn ³ PdAD ⁺	-	-	-	0.4	<0.01

^a The C4 distance between NAD⁺ and the analogue is a measure for the pyridinium shift.

^b k_{cat} values are from table 4.III.

^c Value was obtained from X-ray analysis [13].

^d instead of oxygen, sNAD⁺ has a sulphur atom bound in the side chain of the pyridinium ring.

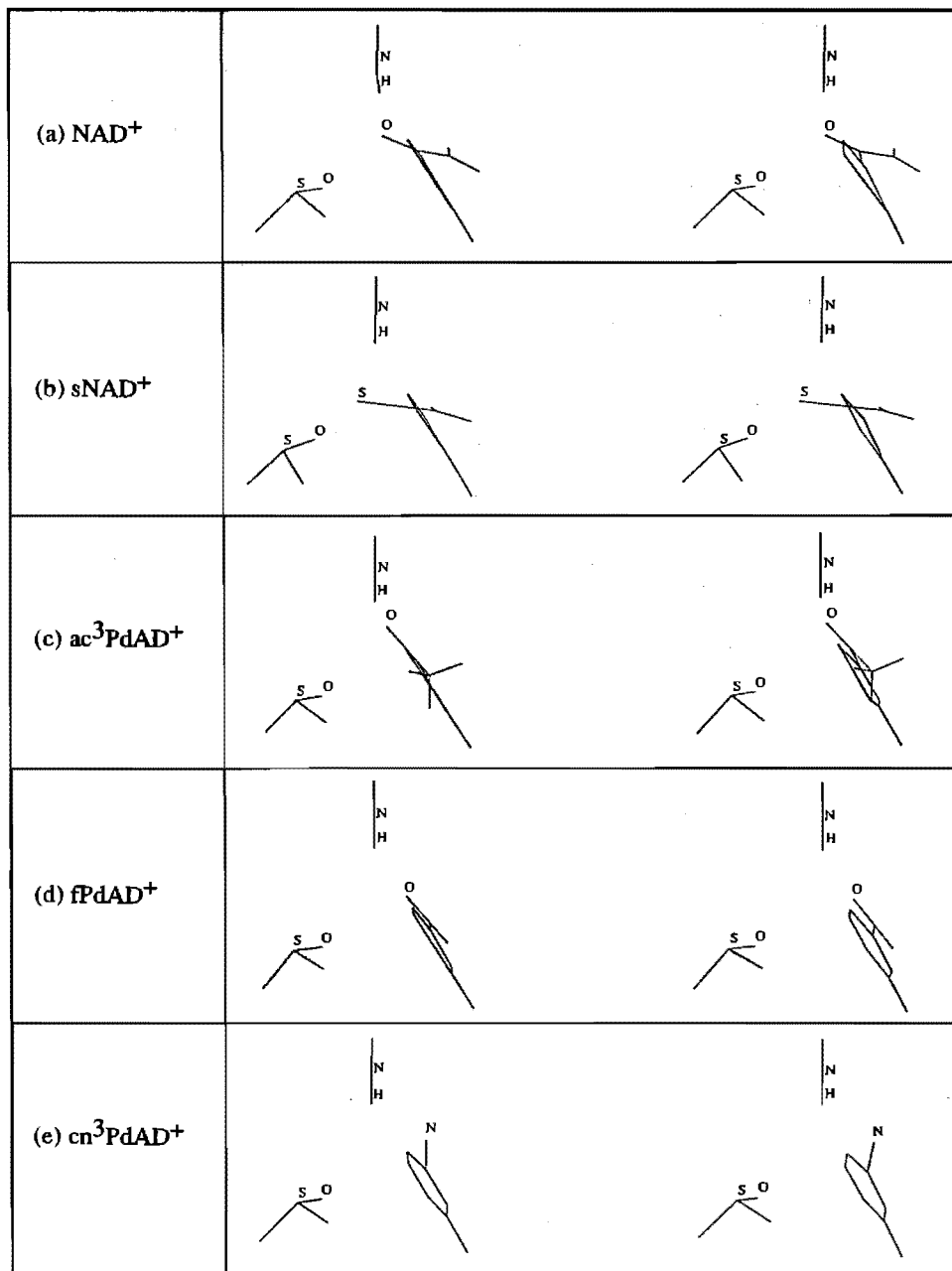


Figure 4.2 Stereodiagrams of the position of the nicotinamide moiety of the optimized NAD⁺ derivatives towards the main chain NH group of Phe 319 and the SO group of the substrate DMSO.

4.3.2 Kinetic studies

Table 4.III summarizes our steady-state kinetic data obtained for NAD^+ and its analogues with isopropanol as substrate, in which the actual hydride transfer becomes rate-limiting (see introduction).

Table 4.III Kinetic parameters derived from equation (4.1) for HLADH with ac^3PdAD^+ , sNAD^+ , fPdAD^+ , cn^3PdAD^+ and NAD^+ and the substrate isopropanol.

Compound	K_a (μM)	K_b (mM)	k_{cat} (rel, %)
NAD^+	37	1.3	1.00 ^a
sNAD^+	249	6.0	4.12
ac^3PdAD^+	309	3.5	2.35
fPdAD^+	261	0.5	0.12
cn^3PdAD^+			<0.01 ^b

^a equals to 0.85 s^{-1} , in accordance with literature data [13].

^b see ref [22,23].

It appears that sNAD^+ and ac^3PdAD^+ are more active than NAD^+ , 4.1 and 2.3 times respectively, whereas fPdAD^+ is less active (i.e., approximately 10 per cent of NAD^+). Finally, it is shown that cn^3PdAD^+ is completely inactive.

In order to compare the kinetic data summarized in table 4.III, the intrinsic reactivities of the compounds, $k_{\text{SO}_2^-}$, as measured by the addition of dithionite anion must also be taken into account (table 4.IV).

4.3.3 Discussion

The reported results permit a correlation to be made between the geometric features of NAD^+ and its analogues in the active site and the measured kinetic data with isopropanol, taking into account the intrinsic reactivities.

Table 4.IV Kinetic data of NAD⁺ and derivatives in the reaction with dithionite and in the enzymatic reduction with isopropanol.

Compound	$k_{\text{cat}}(\text{isoprop})$ (rel)	$k_{\text{SO}_2^-}$ (rel)	ϕ (degrees)
NAD ⁺	1.0	1 ^a	34
sNAD ⁺	4.12	3 ^a	47
ac ³ PdAD ⁺	2.35	22 ^a	6.5
fPdAD ⁺	0.12	16 ^b	9
cn ³ PdAD ⁺	<0.01	32 ^b	-

^a ref [24]: NAD⁺: 47 M⁻¹s⁻¹; ac³PdAD⁺: 1050 M⁻¹s⁻¹; sNAD⁺: 150 M⁻¹s⁻¹.

^b The intrinsic reactivity is calculated from the known linear relationship between the log $k_{\text{SO}_2^-}$ (rate constant) for the dithionite reduction and the redox potential, showing a higher rate of dithionite reduction with increasing potential [24]. With a redox potential of -262 mV [25], for fPdAD⁺ an intrinsic reactivity of about 730 M⁻¹s⁻¹ has been obtained. Similarly a redox potential of -240 mV [22] for cn³PdAD⁺ results in a $k_{\text{SO}_2^-}$ of 1513 M⁻¹s⁻¹ [24].

The high k_{cat} value of sNAD⁺ compared to NAD⁺, which have identical positions of their pyridinium rings, can easily be explained by the large value for the "out-of-plane" orientation and the high intrinsic reactivity (see table 4.IV).

Although the intrinsic reactivity of ac³PdAD⁺ is higher than that of sNAD⁺ (table 4.IV) its enzymatic activity is lower. Since the position of the pyridinium ring of ac³PdAD⁺ only slightly differs from NAD⁺, this observation must be mainly explained by the low "out-of-plane" torsion angle of the acetyl group.

The intrinsic reactivity of fPdAD⁺ is almost equal to that of ac³PdAD⁺, which reflects nicely the equivalence of their "out-of-plane" torsion angles. One should therefore expect about equal activities in the enzyme. Actually the activity of fPdAD⁺ is lower by an order of magnitude (table 4.III). This might be due to the position of its head group not being precisely maintained, as a consequence of the lack of the methyl group (or the NH₂ group) in the side chain; the difference between C4 (ac³PdAD⁺) and C4 (fPdAD⁺) is 0.9 Å (figure 4.3). This is also indicated by the long distance between the carbonyl oxygen and the sulphur atom of DMSO, corresponding to the substrate carbon atom that donates the hydride ion (figure 4.2 and table 4.II).

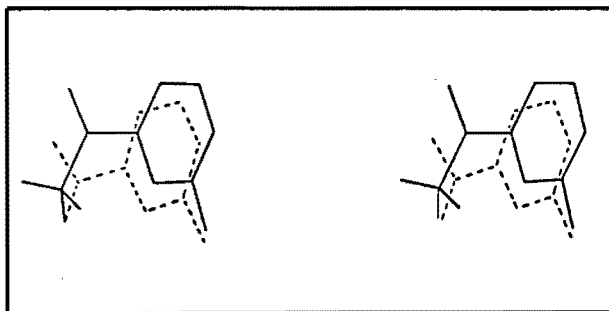


Figure 4.3 Stereodiagram showing the pyridinium position of ac^3PdAD^+ (—) and $fPdAD^+$ (-----).

Most striking are the data obtained with the cyano analogue. According to our calculations the position of the pyridinium ring of cn^3PdAD^+ virtually coincides with that of the pyridinium ring of ac^3PdAD^+ . However, the cyano analogue is practically inactive in the dehydrogenase, notwithstanding its high intrinsic reactivity. The conclusion can be drawn that this is due to the absence of any "out-of-plane" rotation of the CN group (*vide infra*).

The enhancing effect of the carboxamide side chain is ascribed to the δ^- charge of the carbonyl oxygen (-0.28 e.u.), stabilizing the positive charge on C_1 of the substrate in the transition state [26]. In the case of the cyano analogue the cyano group occupies an unfavourable position (figure 4.2), the distance between the δ^- charge of the nitrogen atom and the sulphur atom of the substrate (5.4 Å) being larger than the distance between the δ^+ charge of the carbon atom and the sulphur atom (4.8 Å). The cyano group may therefore even retard the hydride transfer.

4.4 Conclusions

In this chapter, we have demonstrated that the kinetic data obtained with NAD^+ and its analogues can be related to their geometry in the active site of HLADH. Particularly the magnitude of the "out-of-plane" rotation of the carboxamide side chain is decisive.

References

1. Colowick, S.P., Van Eijs, J. and Park, J.M. *Comp. Biochem.* (Florkin and Stoltz, eds) **14** (1966), 38-46.
2. Biellmann, J.F. in "34. Colloquium-Mosbach, Biological Oxidations", Springer-Verlag, Berlin Heiderberg, (1983), 55-61.
3. Biellmann, J.F., Hirth, C.G., Jung, M.J., Rosenheimer, N. and Wrixon, A.D. *Eur. J. Biochem.* **41** (1974), 517-524.
4. Boyer, P.D., Lardy, H. and Myrbäck, K. in "The Enzymes" 2d ed., **7** (1963), 42.
5. Samama, J.P., Marchal-Rosenheimer, N., Biellmann, J.F. and Rossmann, M.G. *Eur. J. Biochem.* **120** (1981), 563-569.
6. Shore, J.D. and Theorell, H. *Eur. J. Biochem.* **2** (1967), 32-36.
7. Shore, J.D. and Brooks, R.L. *Arch. Biochem. Biophys.* **147** (1971), 825-827.
8. Kaplan, N.O., Ciotti, M.M. and Stolzenbach, F.E. *J. Biol. Chem.* **221** (1956), 833-844.
9. Anderson, B.M., Anderson, C.D., Lee, J.K. and Stein, A.M. *Biochemistry* **2** (1963), 1017-1022.
10. Baici, A., Luisi, P.L. and Attanasi, O. *J. Mol. Catalysis* **1** (1975/76), 223-244.
11. Anderson, B.M. and Kaplan, N.O. *J. Biol. Chem.* **234** (1959), 1226-1232.
12. Dalziel, K. and Dickinson, F.M. *Biochem. J.* **100** (1966), 34-46.
13. Eklund, H., Samama, J.P. and Jones, T.A. *Biochemistry* **23** (1984), 5982-5996.
14. Skarzynski, T., Moody, P.C.E. and Wonacott, A.J. *J. Mol. Biol.* **193** (1987), 171-187.
15. Wallén, L. and Branlant, G. *Eur. J. Biochem.* **137** (1983), 67-73.
16. Vorontsov, E.A., Kalacheva, N.I., Lifshits, N.L., Mal'tsev, N.I., Yanina, M.M. and Gurevich, V.M. *Biokhimiya* **44** (1979), 324-331.
17. Fisher, T.L., Vercellotti, S.V. and Anderson, B.M. *J. Biol. Chem.* **248** (1973), 4293-4299.
18. Sund, H. and Theorell, H. *Enzymes* **7** (1962), 25-83.
19. Weiner, P.K. and Kollman, P.A. *J. Comp. Chem.* **2** (1981), 287-303.
20. Weiner, S.J., Kollman, P.A., Case, D.A., Singh, U.C., Ghio, C., Alagona, G., Profeta, S. and Weiner, P.K. *J. Am. Chem. Soc.* **106** (1984), 765-784.
21. Weiner, S.J., Kollman, P.A., Nguyen, D.T. and Case, D.A. *J. Comp. Chem.* **7** (1986), 230-252.

22. Woenckhaus, C. and Jeck, R. in "Coenzymes and Cofactors, Pyridine Nucleotide Coenzymes", (D. Dolphin, O. Avramovic and R. Poulson, eds), John Wiley and Sons, New York, 2A (1987), 449-568.
23. Kazlauskas, R.J. *J. Org. Chem.* **53** (1988), 4633-4635.
24. Blankenhorn, G. and Moore, E.G. *J. Am. Chem. Soc.* **102** (1980), 1092-1098.
25. Scharschmidt, M., Fisher, M.A. and Cleland, W.W. *Biochemistry* **23** (1984), 5471-5478.
26. de Kok, P.M.T., Donkersloot, M.C.A., van Lier, P.M., Meulendijks, G.H.W.M., Bastiaansen, L.A.M., van Hooff, H.J.G., Kanters, J.A. and Buck, H.M. *Tetrahedron* **42** (1986), 941-959.

CHAPTER 5*

MIMICKING THE CONFORMATIONAL CHANGES OF HLADH UPON BINDING OF NAD⁺ AND NAD⁺ FRAGMENTS

Abstract

This chapter describes the simulation of the conformational changes of HLADH upon coenzyme binding. Starting from the X-ray structure of a ternary complex of HLADH/NAD⁺/DMSO, both the apo- and holo-enzyme could be simulated using molecular mechanics. From the comparison of the simulated structures it is clear that the conformational differences are of similar magnitude to those reported earlier based upon superposition of the apo- and holo-enzyme X-ray structures.

Simulation studies with NAD⁺ fragments show that the adenosine part is essential in inducing the required conformational changes to bring the enzyme in its active form. This observation is in accordance with the kinetic studies of Sicsic et al. [13,14].

* N.A. Beijer, L.A.AE. Sluyterman and E.M. Meijer, *J. Comput.-aided Mol. Design*, submitted for publication.

5.1 Introduction

Conformational changes on binding of substrates and ligands are known to play an essential role in the action of several enzymes, both allosteric and non-allosteric. One may wonder whether the energy of binding of substrates and ligands is enough to produce such changes. Computational methods available at present may provide the answer at least as far as the order of magnitude is concerned. In order to simulate the conformational change upon coenzyme binding we have chosen HLADH as a model.

It is known from X-ray analysis that the active form of HLADH is represented by a closed structure. The NAD^+ molecule enters into the binding site in the open form (apo-enzyme) and subsequently induces conformational changes resulting in better binding interactions between enzyme and coenzyme (holo-enzyme). Consequently, the dissociation of the reduced coenzyme is coupled to the opening of the coenzyme binding cleft [1-5].

Chapter 3 described the development of a molecular mechanics model to study in detail the interactions of the coenzyme NAD^+ and its analogues with the enzyme HLADH to understand factors involved in the productive binding between coenzyme and enzyme [6-9].

Here, we report the use of our molecular mechanics model in mimicking conformational changes in HLADH upon binding of NAD^+ and NAD^+ fragments (figure 5.1).

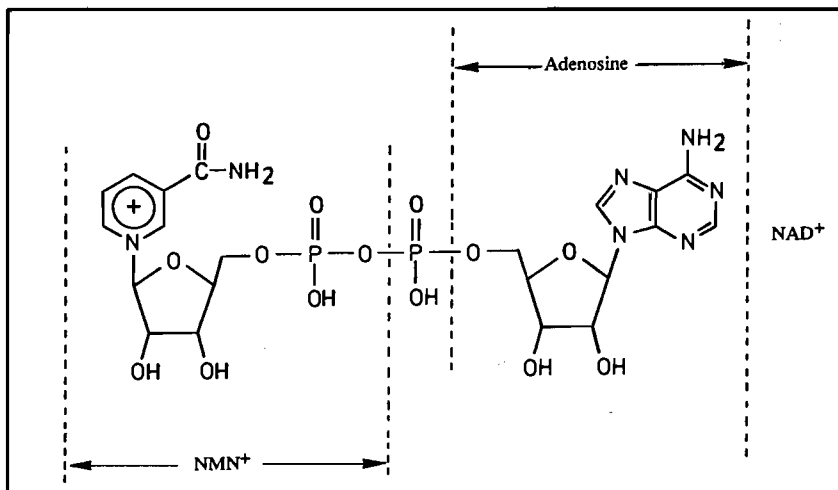


Figure 5.1 Schematic drawing showing the fragments of NAD^+ used (NMN^+ = nicotinamide mononucleotide).

5.2 Procedure for calculational studies

Energy calculations and total energy minimization energies were performed with the AMBER molecular mechanics package (version 3.0) [10] on a VAX 11/785 computer. The starting point for this study has already been described [8] in which the cysteine residues (Cys 46 and 174) were introduced as negatively charged residues. The active site of the holo-HLADH was constructed from X-ray crystallographic data of the ternary complex of HLADH/NAD⁺/DMSO reported by Eklund and coworkers (2.9 Å resolution, crystallographic R factor of 0.22)[1] which was readily retrievable from the Brookhaven Protein Database.

Within a range of 6.0 Å from the coenzyme 44 amino acids were taken into account to represent the active site (see appendix B). During the minimization, we permitted NAD⁺, DMSO and 20 of the 44 amino acids surrounding the active site to move freely (i.e., residues Cys 46, Arg 47, Ser 48, His 51, Val 222, Asp 223, Ile 224, Asn 225, Arg 271, Thr 274, Ile 291, Val 292, Gly 293, Val 294, Pro 295, Gly 316, Ala 317, Ile 318, Phe 319 and Gly 320). Permitting more amino acids to move freely would require excessive calculation time. The minimization procedure to obtain the simulated apo-enzyme geometry has been carried out analogously to that of the holo-enzyme.

The NAD⁺ fragments were constructed from the corresponding parts in the X-ray NAD⁺ structure (figure 5.1). Minimizations were carried out following the methodology described before.

All minimizations were performed until the RMS gradient value of the energy was less than 0.1 kcal.Å⁻¹, using the distance-dependent dielectric constant and treating all CH, CH₂ and CH₃ groups as united atoms. Atomic charges were calculated using the MNDO semi-empirical molecular orbital method. Most harmonic force constants were obtained directly from literature or extrapolated [11,12]. The dihedral torsion angle barrier for the carboxamide "out-of-plane" orientation was chosen as described previously (chapter 3).

Figures were obtained using Chem-X (January 1990 update, copyright Chemical Design Oxford, Ltd. Oxford).

5.3 Results and discussion

5.3.1 Binding of NAD^+

First we simulated the holo-enzyme starting from the X-ray ternary complex. Figure 5.2 shows the conformation of the amino acids of the holo-enzyme compared to the X-ray analysis. Roughly the same conformation of the cage was obtained. Among other data, table 5.I summarizes the conformational parameters of the NAD^+ geometry.

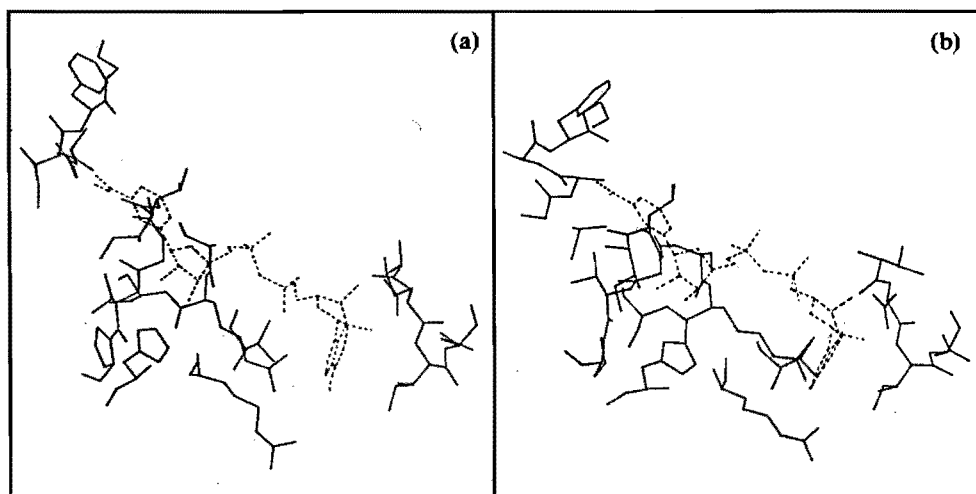


Figure 5.2 Conformation of the cage of the 20 amino acids which were allowed to move freely, (a) according to X-ray analysis and (b) after energy minimization. The geometry of NAD^+ is represented by the broken line.

The calculation was repeated with the omission of NAD^+ . Figure 5.3 visualizes the conformation of the amino acids of the simulated apo-enzyme compared to the simulated holo-enzyme.

Although the model is a simplified one and the AMBER calculations have their limitations, there are similarities in which amino acids are significantly displaced on binding of NAD^+ and which one's not, compared with the X-ray results (table 5.II). This shows the qualitative usefulness of our molecular mechanics approach.

Table 5.1 Conformational parameters (degrees) of energy-refined NAD^+ , NMN^+ and NMN^+ with adenosine. 20 of the 44 amino acids of the chosen active site were kept free to move. Nomenclature of the coenzyme torsion angles is the same as that used before (chapter 3).

Compound	ϕ	χ_A	γ_A	β_A	α_A	ζ_A	ζ_N	α_N	β_N	γ_N	χ_N
NAD^+	22	268	292	105	86	53	250	69	173	53	258
NMN^+	33							65	185	55	263
NMN^+ + Adenosine	20	273	311					67	180	56	257

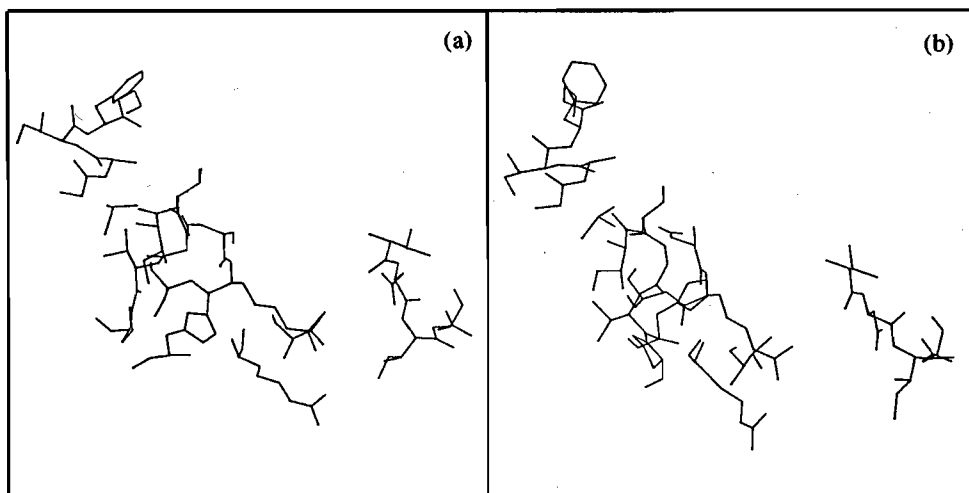


Figure 5.3 Conformation calculated in the presence of NAD^+ (a, equal to figure 5.2; NAD^+ not drawn for the sake of clarity) and (b) conformation calculated in the absence of NAD^+ .

Table 5.II Displacements (Å) of the C_α atoms of some amino acid residues of the calculated holo-enzyme versus the calculated apo-enzyme and the X-ray holo-enzyme versus X-ray apo-enzyme (N = nicotinamide moiety; A = adenosine moiety).

Amino acid residue	interacting coenzyme moiety	displacement calc. enzyme	displacement X-ray enzyme
Cys 46	nicotinamide	1.0	1.6
Arg 47	ribose/phosphate (N)	1.1	1.6
His 51	ribose (N)	3.1	2.9
Asp 223	ribose (A)	1.1	0.9
Ile 224	adenine	1.2	1.1
Gly 293	nicotinamide	1.8	1.7
Val 294	nicotinamide/ribose	2.0	1.8
Pro 295	ribose (N)	4.6	2.8

Without NAD⁺ the coenzyme cavity is clearly enlarged whereas it becomes smaller after NAD⁺ binding owing to hydrogen bonding with the surrounding amino acids. Particularly the side chains of Arg 271 and Ile 224, situated at the adenine-binding side of the active site, are involved in the change of the conformation upon coenzyme binding and dissociation. This is illustrated by the distance of 8.0 Å between the side chains of Arg 271 and Ile 224 in the apo-enzyme, whereas after NAD⁺ binding it is reduced to 3.4 Å. The simulated conformational change of the NAD⁺-binding site also coincides with earlier observations reported in literature [1-3]. Side chain movements even exceed those of C_α atoms, for example Val 294 (C_{γ1}) 4.4 Å and Pro 295 (C_β) 4.6 Å (in the X-ray structure those values are 5.1 Å and 4.1 Å, respectively).

5.3.2 Binding of NAD⁺ fragments

In order to investigate which part of NAD⁺ is responsible for the observed and simulated conformational changes, we simulated the NAD⁺-binding site in the presence of NMN⁺ alone and combined with adenosine (figures 5.4 and table 5.I).

From figures 5.4a it is clear that NMN⁺ alone is not able to induce

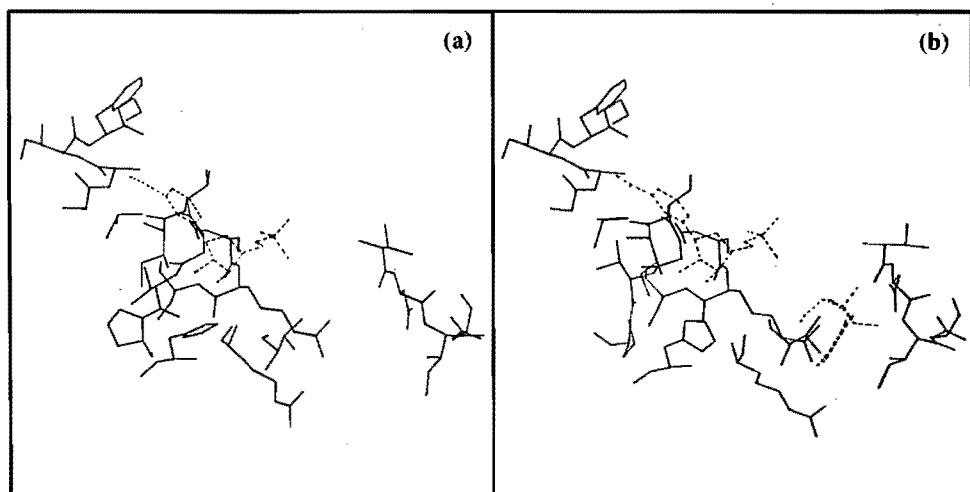


Figure 5.4 Conformation calculated in the presence of NMN^+ (a) and (b) in the presence of NMN^+ and adenosine. Those amino acids which were kept free to move during the minimizations are drawn. Broken lines represent the coenzyme fragments.

Table 5.III Shifts (\AA) of C_α atoms of some amino acid residues of calculated enzyme complexes versus calculated apo-enzyme.

coenzyme moiety	interacting amino acid	complexes		
		NMN^+	NMN^+ + adenosine	NAD^+
nicotinamide	Cys 46	0.9 ☆	1.0	1.0
nicotinamide	Gly 293	2.0 ☆	1.9	1.8
nicotinamide/ribose	Val 294	1.1	2.0 ★	2.0
ribose (N)	His 51	2.9 ☆	3.0	3.1
ribose (N)	Pro 295	3.3	4.6 ★	4.6
ribose/phosphate (N)	Arg 47	0.9 ☆	1.0	1.1
ribose (A)	Asp 223	0.1	0.8 ★	1.1
adenine	Ile 224	0.1	1.3 ★	1.2

☆ shift equal to those of NAD^+ .

★ shifts caused by the additional presence of an adenosine containing fragment.

the required conformational changes. After addition of the missing adenosine part in the calculations, however, conformational changes do occur (figures 5.4b) comparable to those observed with the holo-enzyme (table 5.III). Besides, although there is no direct contact between the two NAD^+ fragments owing to the lack of one phosphate group, the adenosine affects the conformation of the NMN^+ in maintaining most of its conformational angles closer to those of NAD^+ than those of NMN^+ alone (table 5.I).

From these results it can be inferred that the adenosine part of NAD^+ is essential in triggering the conformational changes. This is reminiscent of an allosteric effect.

This conclusion is in accordance with the results of Sicsic et al. [13,14], who showed in kinetic experiments with alcohol dehydrogenase that only a very low level of activity is retained using NMN^+ as a cofactor (table 5.IV). In the presence of adenosine the activity with NMN^+ is substantially increased (6 times).

Table 5.IV Kinetic data of NAD^+ and NAD^+ fragments with HLADH obtained by Sicsic et al. [13,14].^a

Compound	V_{\max} (rel, %)
NAD^+	100
NMN^+	5
NMN^+ + adenosine	30

^a Unfortunately, we were not able to reproduce the kinetic experiments with the NAD^+ fragments as published by Sicsic et al. [13,14].

Based upon these kinetic results and our modelling experiments, we propose that the adenosine part of NAD^+ is of vital importance for the coenzyme activity by inducing the required conformational change in the apo-enzyme.

5.4 Conclusions

In this chapter we have described a molecular mechanics approach to mimic the conformational changes occurring in HLADH upon coenzyme binding. Although the

present results are no more than a first approach of the problem, they indicate that NAD⁺-enzyme interactions are sufficient to trigger the kind of conformational change observed in HLADH on coenzyme binding. From the study with NMN⁺ we can conclude that an adenosine part is necessary to induce the conformational change of the enzyme to bring it in its active form.

References

1. Eklund, H., Samama, J.P. and Jones, T.A. *Biochemistry* 23 (1984), 5982-5996.
2. Eklund, H. and Brändén, C.I. *Biological Macromolecules and Assemblies* (1987), 73-142.
3. Eklund, H. and Brändén, C.I. in "Coenzymes and Cofactors, Pyridine Nucleotide Coenzymes" (D. Dolphin, O. Avramovic and R. Poulson, eds) John Wiley and Sons, New York, 2A (1987), 51-98.
4. Eklund, H. and Brändén, C.I. *J. Biol. Chem.* 254 (1979), 3458-3461.
5. Colonna-Cesari, F., Perahia, O., Karplus, M., Eklund, H., Brändén, C.I. and Tapia, O. *J. Biol. Chem.* 261 (1986), 15273-15280.
6. de Kok, P.M.T., Beijer, N.A., Buck, H.M., Sluyterman, L.A.AE. and Meijer E.M. *Recl. Trav. Chim. Pays-Bas* 107 (1988), 355-361.
7. de Kok, P.M.T., Beijer, N.A., Buck, H.M., Sluyterman, L.A.AE. and Meijer E.M. *Eur. J. Biochem.* 175 (1988), 581-585.
8. Beijer, N.A., Buck, H.M., Sluyterman, L.A.AE. and Meijer E.M. *Biochim. Biophys. Acta* 1039 (1990), 227-233.
9. Beijer, N.A., Buck, H.M., Sluyterman, L.A.AE. and Meijer E.M. *Ann. N. Y. Acad. Sci.* (1990) in press.
10. Weiner, P.K. and Kollman, P.A. *J. Comp. Chem.* 2 (1981), 287-303.
11. Weiner, S.J., Kollman, P.A., Case, D.A., Singh, U.C., Ghio, C., Alagona, G., Profeta, S. and Weiner, P.K. *J. Am. Chem. Soc.* 106 (1984), 765-784.
12. Weiner, S.J., Kollman, P.A., Nguyen, D.T. and Case, D.A. *J. Comp. Chem.* 7 (1986), 230-252.
13. Sicsic, S., Durand, P., Langrené, S. and Le Goffic, F. *FEBS Lett.* 176 (1984), 321-324.
14. Sicsic, S., Durand, P., Langrené, S. and Le Goffic, F. *Eur. J. Biochem.* 155 (1986), 403-407.

CHAPTER 6*

SIMULATION OF POLYETHYLENE GLYCOL BOUND NAD⁺

Abstract

Polyethylene glycol bound nicotinamide adenine dinucleotide (PEG-NAD⁺) has been successfully employed in the continuous production of L-amino acids from the corresponding α -keto acids by stereospecific reductive amination.

Using molecular mechanics to simulate the geometry of PEG-NAD⁺ in the active site of HLADH, we are now able to rationalize the activity of PEG-NAD⁺.

* N.A. Beijer, S.A.M. Vanhommerig, L.A.AE. Sluyterman and E.M. Meijer, *Recl. Trav. Chim. Pays-Bas*, special issue "Biocatalysis in organic chemistry", submitted for publication.

6.1 Introduction

A number of synthetically useful enzymatic reactions require cofactors such as NAD^+ . These cofactors are too expensive to be used as stoichiometric reagents. Regeneration of the cofactors from their reaction by-products is thus required to make the process economical. Many procedures have been suggested to achieve efficient coenzyme recycling, including enzymatic and non-enzymatic methods [1]. One of the systems investigated, the enzyme membrane reactor concept developed by Wandrey and co-workers [2,3], shows commercially attractive features. For example, continuous production of L-amino acids from the corresponding α -keto acids by stereospecific reductive amination has been achieved with little cofactor consumption in a membrane reactor in which NAD^+ is covalently linked to polyethylene glycol (PEG- NAD^+ ; figure 6.1) [4]. However, the surprising observation that PEG-10,000- NAD^+ displays a similar activity in the enzymatic reaction as native NAD^+ , is not yet understood at the molecular level.

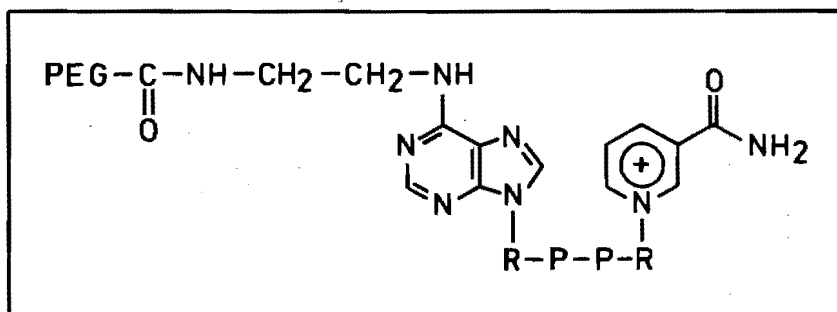


Figure 6.1 Structure of NAD^+ covalently linked to polyethylene glycol.

In the preceding chapters we have described the development of a molecular mechanics model to study in detail the interactions of NAD^+ and a number of analogues with HLADH in order to understand the essential factors involved in the productive binding between coenzyme and apo-enzyme [5-8]. The results demonstrated that the enzymatic activity of NAD^+ and its analogues can be related to the simulated coenzyme geometry in the ternary complex.

We now report that the AMBER molecular mechanics model enables us to rationalize the enzymatic activity of PEG- NAD^+ .

6.2 Procedure for calculational studies

Energy calculations and total energy minimization energies were performed with the AMBER molecular mechanics package (version 3.0) [9] on a VAX 11/785 computer.

The procedure is adopted directly from the method described in previous chapters [5-8]. The starting point for the positioning of PEG-NAD⁺ in HLADH is the crystallographic structure of the ternary complex of HLADH with NAD⁺ and DMSO [10]. Since the enzyme is too large to be involved completely in the calculations, we constructed a cage of 44 amino acids to represent the active site of HLADH.

The three-dimensional starting structure of PEG-NAD⁺ was constructed from the X-ray NAD⁺ geometry to which we linked PEG residues using Chem-X (April 1989 update, copyright Chemical Design Oxford Ltd, Oxford). Due to the boundaries of the chosen protein cage, the coupling of only four PEG residues to the exocyclic adenine-NH₂ group was considered to be relevant.

All energy minimizations were performed until the RMS gradient value of the energy was less than 0.1 kcal.Å⁻¹, using the distance-dependent dielectric constant and treating all CH, CH₂ and CH₃ groups as united atoms.

Atomic charges were calculated using the MNDO semi-empirical molecular mechanics orbital method. Most harmonic force constants were obtained directly from the literature or extrapolated [11,12]. The dihedral torsion angle barrier for the carboxamide orientation was chosen as described in detail in chapter 3 [7].

6.3 Results and discussion

The geometry of the energy-minimized PEG-NAD⁺ relative to the energy-refined geometry of NAD⁺ is presented in figure 6.2. Neither the zinc ion nor the amino acids are depicted since they were kept invariant during the initial calculations [5]. Table 6.I summarizes the numerical values of the torsion angles of the PEG-NAD⁺ and NAD⁺ geometries.

The results show that PEG-NAD⁺ binds in a similar way as NAD⁺. Although the adenosine part is moved somewhat away (1.6 Å) due to the presence of the PEG chain, the nicotinamide ring occupies the same position. Since the geometry of the latter largely determines the activity of the coenzyme in the enzymatic reaction [7], it can be expected that the activities of PEG-NAD⁺ and native NAD⁺ are indeed comparable.

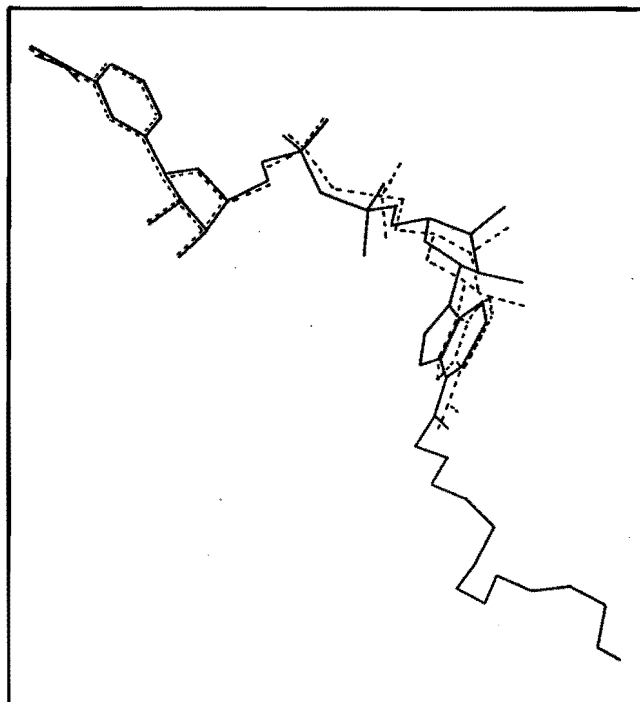


Figure 6.2 Visualization of the energy-minimized PEG-NAD⁺ geometry (—) compared to the energy-refined geometry of the NAD⁺ coenzyme (-----) in a fixed core of amino acids.

Table 6.1 Conformational parameters (degrees) of the energy-refined PEG-NAD⁺ and NAD⁺ geometry. Nomenclature of the coenzyme torsion angles is the same as that used before (N = nicotinamide side of NAD⁺; A = adenine side of NAD⁺).

Compound	χ_A	γ_A	β_A	α_A	ζ_A	ζ_N	α_N	β_N	γ_N	χ_N
Fixed core:										
PEG-NAD ⁺	244	300	172	64	80	198	57	195	55	271
NAD ⁺	253	292	153	65	91	201	57	185	53	271
Partly mobile core:										
PEG-NAD ⁺	267	293	109	83	58	242	66	180	50	253
NAD ⁺	268	292	105	86	53	250	69	173	53	258

It is known that conformational changes in the apo-enzyme occur on binding of the coenzyme. In a second set of modelling experiments, we therefore allowed 20 amino acids surrounding the adenosine structure to move freely during the energy minimization procedures. Figure 6.3 shows a shift of the pyridinium ring, whereas the position of the adenosine unit is now virtually identical to that of native NAD^+ . Closer inspection of the geometric data (table 6.II) reveals that the relatively small shift of the pyridinium C4-atom (0.4 Å) away from the substrate might be compensated by the increased torsion angle (from 22° to 47°) between the carboxamide side chain and the pyridinium ring ("out-of-plane" rotation).

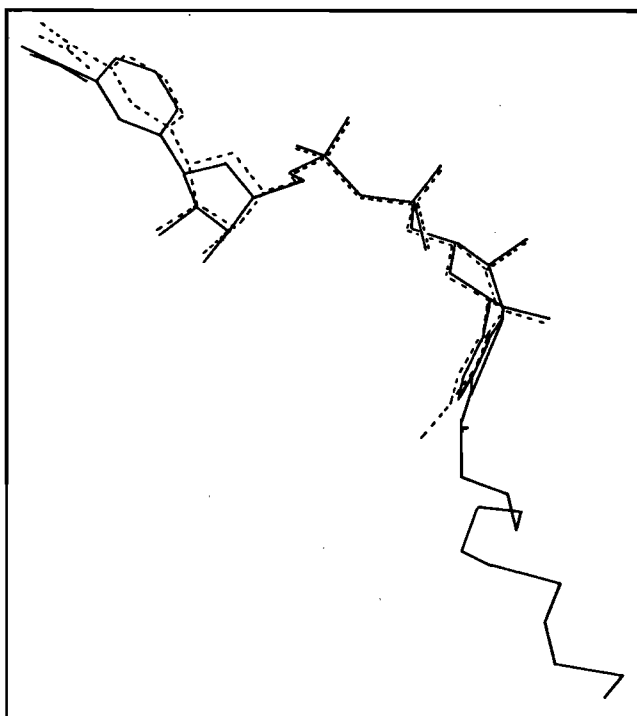


Figure 6.3 The energy-minimized PEG-NAD⁺ geometry (—) compared to the energy-minimized geometry of the NAD⁺ coenzyme (-----) in a core of amino acids from which 20 residues were allowed to move during the minimization.

In a previous chapter (chapter 4, [7]) we have argued qualitatively that an increase in torsional angle enhances the reaction rate, the carbonyl oxygen aiding the transfer of the hydride ion from the substrate to the pyridinium moiety; it is evident that in the present

case the distance between the carbonyl oxygen and the sulphur of the substrate analogue DMSO is 0.3 Å shorter than in the case of NAD⁺ (table 6.II).

Table 6.II Geometric data of energy-refined PEG-NAD⁺ and native NAD⁺ in a partly mobile core of amino acids in relation to kinetic data [2,3].

Compound	ϕ (deg)	N(Phe 319)- O(C(O)NH ₂) (Å)	S(DMSO)- O(C(O)NH ₂) (Å)	C4- C4(NAD ⁺) ^a (Å)	k_{cat} ^b (rel)
NAD ⁺	22	3.5	4.4	-	1
PEG-NAD ⁺	47	2.8	4.1	0.4	~1

^a The C4 distance between NAD⁺ and PEG-NAD⁺ is a measure of the pyridinium shift.

^b So far the reported kinetic data for PEG-NAD⁺ [2,3] were essentially obtained with amino acid dehydrogenases. We also found HLADH to be active with PEG-NAD⁺.

6.4 Conclusions

In conclusion, this study shows, for the first time, that based upon molecular mechanics calculations the activity of PEG-NAD⁺ in enzymatic reactions (dehydrogenases) can be rationalized.

References

1. Wang, S.S. and King, C.K. *Adv. Biochem. Engin.* 12 (1979), 119-146.
2. Wichmann, R., Wandrey, C., Bückmann, A.F. and Kula, M.R. *Biotechn. Bioeng.* 23 (1981), 2789-2802.
3. Wandrey, C. and Wichmann, R. *Biotechnology series 5* (1985), 177-208.
4. Wandrey, C. in "Proceedings 4th European Congress on Biotechnology", (O.M. Neijssel, R.R. van der Meer and K.Ch.A.M. Luyben, eds), Elsevier, Amsterdam, 4 (1987), 171-188.

5. De Kok, P.M.T., Beijer, N.A., Buck, H.M., Sluyterman, L.A.AE. and Meijer, E.M. *Recl. Trav. Chim. Pays-Bas* **107** (1988), 355-361.
6. De Kok, P.M.T., Beijer, N.A., Buck, H.M., Sluyterman, L.A.AE. and Meijer, E.M. *Eur. J. Biochem.* **175** (1988), 581-585.
7. Beijer, N.A., Buck, H.M., Sluyterman, L.A.AE. and Meijer, E.M. *Biochim. Biophys. Acta* **1039** (1990), 227-233.
8. Beijer, N.A., Buck, H.M., Sluyterman, L.A.AE. and Meijer, E.M. *Ann. N. Y. Acad. Sc.*, (1990) in press.
9. Weiner, P.K. and Kollman, P.A. *J. Comp. Chem.* **2** (1981), 287-303.
10. Eklund, H., Samama, J.P. and Jones, T.A. *Biochemistry* **23** (1984), 5982-5996.
11. Weiner, S.J., Kollman, P.A., Case, D.A., Singh, U.C., Ghio, C., Alagona, G., Profeta, S. and Weiner, P.K. *J. Am. Chem. Soc.* **106** (1984), 765-784.
12. Weiner, S.J., Kollman, P.A., Nguyen, D.T. and Case, D.A. *J. Comp. Chem.* **7** (1986), 230-252.

CHAPTER 7

SIMULATION OF THE COENZYME GEOMETRY IN HLADH WITH SINGLE AMINO ACID SUBSTITUTIONS

Abstract

A range of mutated HLADH's have been simulated using molecular mechanics in order to select those amino acid residues which substantially affect the coenzyme geometry. The methodology developed may be helpful in selecting targets for site-directed mutagenesis in order to engineer HLADH genetically so as to optimize the interaction of the apo-enzyme and coenzyme.

Due to their influence on the coenzyme positioning Val 292, Ala 317, Phe 319 and Arg 369 seem to be first choice candidates for site-directed mutagenesis.

7.1 Introduction

In the previous chapters it was shown that AMBER molecular mechanics calculations are very useful in studying the interactions of several NAD^+ derivatives with HLADH. Relevant geometric properties of these coenzymes in relation to their enzymatic reactivities have emerged.

In this chapter we describe our investigations concerning the simulation of a selected number of amino acid substitutions in the apo-enzyme and the effects of these "mutations" on the previously reported coenzyme geometries.

Since the HLADH gene has not yet been cloned completely (work in our laboratory is in progress [1]), we have based our studies on kinetic data of mutated yeast ADH in order to validate our AMBER model. It is known that the subunit conformation and the catalytic mechanism of the yeast and horse liver enzyme are largely similar [2,3].

After establishing the usefulness of the model, a range of mutated HLADH's have been simulated in order to select those amino acid residues which substantially affect the coenzyme geometry.

The methodology developed may be helpful in selecting targets for site-directed mutagenesis in order to engineer HLADH genetically in such a way that eventually improved interactions with simple coenzyme analogues can be produced.

7.2 Procedure for calculational studies

Energy calculations and total energy minimization energies were performed with the AMBER molecular mechanics package (version 3.0) [4] on a VAX 11/785 computer. The procedure is adopted directly from the method described in chapter 3.

Substitutions of amino acids were carried out using Chem-X (April 1989 update, copyright Chemical Design Oxford Ltd, Oxford).

During the energy minimizations the residues which are close to the substituted residue were allowed to move with the use of the "Belly" option in AMBER. These "free" residues are presented in table 7.I.

Table 7.1 Amino acids which have been subjected to substitution in this study and those residues in the near area of the substituted residue which are allowed to move during the energy minimization. Their full names are listed in appendix B.

Amino acid to be substituted	"Free" amino acid residues
Cys 46	46-48
Arg 47	46-48
His 51	46-48, 51, 56, 57
Glu 68	67, 68, 369
Cys 174	173-175, 178
Val 203	200-204
Asp 223	222-225, 228
Lys 228	222-225, 228
Val 292	291-295
Ala 317	316-320
Phe 319	316-320
Arg 369	369

7.3 Results and discussion

First, we started from known data concerning to yeast ADH in order to demonstrate the suitability of our AMBER model. Three different replacements, i.e., Val 203 by Ala [5], His 51 by Gln [6] and Glu 68 by Gln [7] have been studied in HLADH. The calculated native enzyme-coenzyme complex is compared with the simulated mutant complex. Conformational changes are translated to coenzyme geometries which are in turn related to activities reported in the literature for yeast ADH.

7.3.1 Substitution of Val 203

In yeast ADH, the *syn* conformation of NAD⁺ is sterically obstructed by a leucine residue at position 182 [5]. Altering this residue to alanine, by site-directed mutagenesis, most of the steric obstruction is removed, resulting in a decrease of the catalytic activity by 70% [5].

In HLADH, valine 203 was found in the corresponding position. Given the results with yeast ADH, we studied the substitution of Val 203 by Ala and its influence on the NAD⁺ geometry.

During the energy minimization, the amino acids in the immediate surroundings of the substitution, i.e., amino acid residues Leu 200 to Gly 204, were allowed to move. In order to visualize the effect of the substitution on the NAD⁺ geometry, the energy-minimized NAD⁺ geometry both in the native as well as in the mutant enzyme are depicted in figure 7.1. Table 7.II summarizes, among other data, the numerical values of the most important torsion angles. The glycosidic bond χ_N of NAD⁺ has changed from 271° to 240°, showing that due to the substitution the steric obstruction exerted by residue 203 is partly removed. Probably, the strong hydrogen bonding of the pyridinium side chain with Val 292, Ala 317 and Phe 319 prevent a complete rotation.

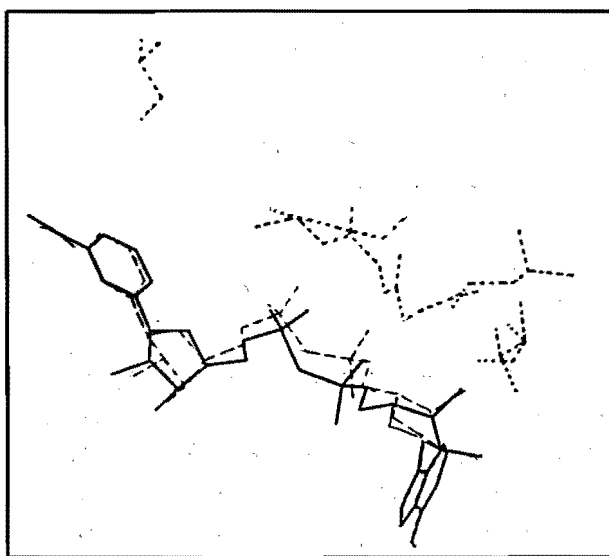


Figure 7.1 Visualization of the energy-minimized NAD⁺ geometry in the Val203Ala mutant (—) of HLADH versus to the energy-minimized NAD⁺ geometry in the native enzyme (---). Only those amino acids which were allowed to move during the minimizations (Leu 200, Gly 201, Gly 202, Val203Ala, Gly 204) are drawn (----).

Some of the relevant geometric data of the pyridinium moiety are also shown in table 7.II. In the case of the Val 203 substitution the pyridinium ring is shifted only 0.2 Å away. Other factors have not changed significantly.

Since the positioning of the pyridinium ring is the most important factor in determining the enzymatic activity, we may conclude that, despite the displacement of the phosphate bridge, the reduction of enzyme activity observed in the Leu203Ala mutant of

yeast ADH can be tentatively explained by the simulated rotation around the glycosidic bond, through which the pyridinium ring occupies a somewhat less favourable position.

Table 7.II Geometric data of the energy-refined NAD⁺ in the native enzyme and some mutants.

substitution	ϕ (deg)	χ_N (deg)	N(Phe 319)- O(C(O)NH ₂) (Å)	S(DMSO)- O(C(O)NH ₂) (Å)	C4(native)- C4(mutant) ^a (Å)	k _{cat} ^b (rel)
none	34	271	2.9	4.2	-	1
Val203Ala	35	240	2.9	4.0	0.2	1/3
His51Gln	30	250	2.8	4.4	0.4	1/27
Glu68Gln	34	271	2.9	4.0	0.4	1/30

^a The C4 distance between NAD⁺ in the native and in the mutant enzyme is a measure for the pyridinium shift.

^b Enzymatic activity determined with yeast ADH.

7.3.2 Substitution of His 51

It is known that the replacement of His 51 in yeast ADH by glutamine (Gln) reduces the activity 27-fold [6]. In HLADH there is also a histidine residue at position 51. His 51 is known to bind both hydroxy groups of the nicotinamide ribose ring. Substitution of His 51 might therefore result in rather large movements of the ribose ring.

Geometric data of NAD⁺ bound in the active site of the His51Gln mutant of HLADH are shown in table 7.II. Figure 7.2 shows the effect of the His51Gln mutation on the energy-refined NAD⁺ geometry compared to its position in the native enzyme.

The ribose ring is clearly displaced after replacement of His by Gln (0.9 Å). The observed shift of the pyridinium ring (table 7.II) can be seen as a correction arising from the movement of the ribose ring.

The large difference in activity (table 7.II) between the Leu203Ala mutant and the His51Gln mutant of yeast ADH might be explained by assuming that with the latter mutant the pyridinium ring is more rotated (C4 shift is 0.4 Å instead of 0.2 Å for the simulated Val203Ala mutant of HLADH).

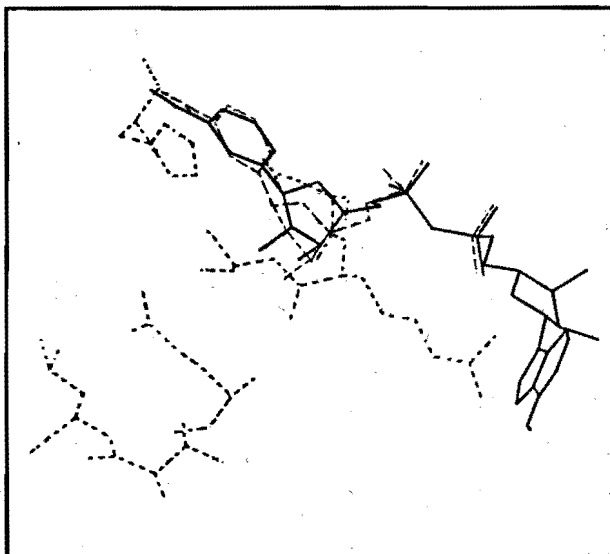


Figure 7.2 Representation of the energy-refined NAD⁺ geometry in the His51Gln mutant (—) of HLADH compared to the energy-minimized NAD⁺ geometry in the native enzyme (---). Only the amino acid residues which were kept free to move (Cys 46, Arg 47, Ser 48, His 51Gln, Thr 56 and Leu 57) are drawn (-----).

7.3.3 Substitution of Glu 68

The substitution of Glu 68 by Gln differs from the previous mutations in that a charged amino acid residue has been replaced by its uncharged analogue. It has been postulated that the accumulation of negatively charged residues (Cys 46, Cys 174, Glu 68 and Asp 49) may serve to modulate the polarizing effect of the metal (Zn) in order to facilitate hydride transfer to NAD⁺ and to prevent substrates and products from binding too tightly [7].

To evaluate the role of the conserved carbonyl groups, Glu 68 has been replaced by glutamine (Gln). The Glu68Gln mutant of the yeast enzyme shows a 30-fold lower activity [7].

Both in yeast and in horse liver ADH, Glu 68 is not directly hydrogen bonded to NAD⁺, but it exerts its influence via Arg 369 with which Glu 68 forms double hydrogen

bonds. The most important geometric data of NAD^+ in the "mutated" HLADH have been summarized in table 7.II.

Figure 7.3 shows the geometry of energy-refined NAD^+ in the mutant compared to that in the native enzyme. The displacement of both the nicotinamide ring and the ribose ring as a result of changed interactions of Arg 369 with NAD^+ is noteworthy.

This might explain the 30 times lower activity measured with the Glu68Gln mutant of

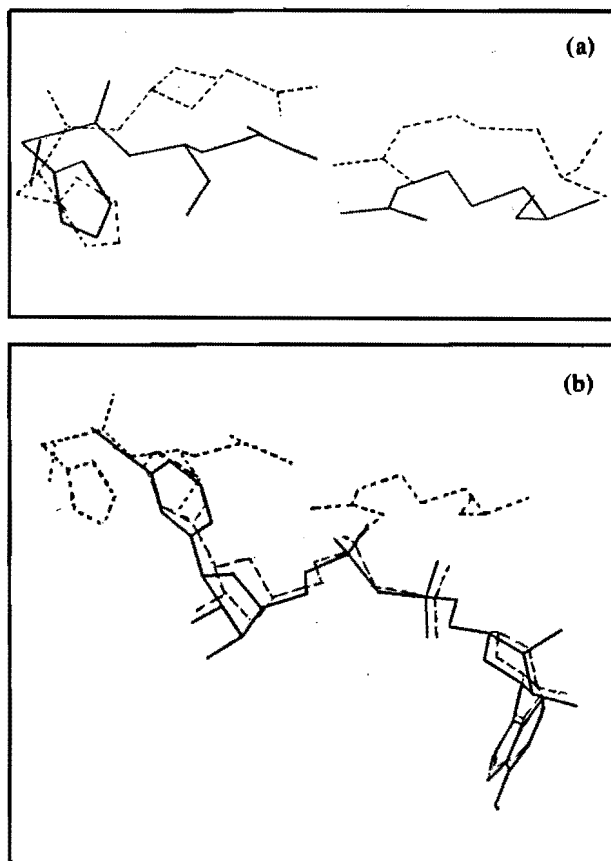


Figure 7.3 (a) The effect of the Glu68Gln mutation on the "free" amino acid residues His 67, Glu68 (Gln) and Arg 369, before (-----) and after (—) substitution of Glu 68, and (b) the comparison of the energy-minimized NAD^+ geometry in the Glu68Gln mutant (—) of HLADH versus the energy-minimized NAD^+ geometry in the native HLADH (---). Only those amino acids which were kept free to move (His 67, Glu68Gln and Arg 369) are drawn (-----).

yeast ADH compared to the native enzyme. Since the calculated perturbations of the NAD^+ geometry in the HLADH mutant are rather similar to those in the His51Gln mutant (especially the shift of the pyridinium ring), it is not surprising that the measured activities are also of the same level (table 7.II).

In conclusion, the results of the simulations of the coenzyme geometry in the three simulated mutants of HLADH show that we are able to rationalize the kinetic data obtained with the corresponding mutants of yeast ADH.

7.3.4 Simulation of other single amino acid substitutions in HLADH

The foregoing studies indicate that single amino acid substitutions can be modelled effectively. Therefore a number of other amino acids interacting with NAD^+ were chosen as targets for substitution by, firstly, the smallest amino acid glycine. This investigation should be regarded as a first step on the way to our ultimate goal, i.e., the optimization of the interaction of coenzyme analogues with the HLADH apo-enzyme.

Influences of these "mutations" on the coenzyme geometry have been elaborated and are summarized in tables 7.III.

Table 7.III Numerical values of the energy-refined NAD^+ geometry in the native enzyme and in some mutants.

Substitution	ϕ (deg)	N(Phe 319)- O(C(O)NH ₂) (Å)	S(DMSO)- O(C(O)NH ₂) (Å)	C4(NAD^+ , mutant)- C4(NAD^+ , native) (Å)
None	34	2.9	4.2	-
Cys46Gly	38	2.9	3.8	0.28
Arg47Gly	37	2.9	4.2	0.19
His51Gly	30	2.8	4.2	0.34
Glu68Gly	32	2.9	4.0	0.08
Cys174Gly	38	2.9	4.0	0.17
Val203Gly	35	2.9	4.0	0.17
Asp223Gly	38	3.0	4.2	0.06
Lys228Gly	32	2.9	4.2	0.09
Val292Gly	51	2.9	4.2	0.09
Ala317Gly	40	2.8	4.0	0.08
Phe319Gly	33	2.9	4.2	0.20
Arg369Gly	27	2.9	4.3	0.45

In chapter 4 we have already argued that an increase in torsion angle of the carboxamide side chain of NAD^+ enhances the reaction rate, the carbonyl oxygen aiding the transfer of the hydride ion from the substrate to the pyridinium moiety.

In this respect, two substitutions which first catch the eye (table 7.III) are the replacements of Val 292 and Arg 369 by glycine. The first mutation leads to an increase of the "out-of-plane" rotation from 34° to 51° . On the other hand the Arg369Gly mutant of HLADH shows an overall bad fit of the coenzyme, expressed by the low ϕ and the large shift of the pyridinium ring, indicating the importance of the conserved Arg 369 residue in all dehydrogenases. Most other "mutations" appear to be less significant regarding the geometry of NAD^+ .

Further we worked out the Val 292 substitution through binding studies of NAD^+ analogues. Results of the simulations are given in table 7.IV.

Table 7.IV Comparison of geometric data of energy-minimized NAD^+ and NAD^+ analogues in the active site of native and mutated HLADH.

substitution	coenzyme	ϕ (deg)	N(Phe 319)- O(C(O)R) (Å)	S(DMSO)- O(C(O)R) (Å)	C4(coenzyme)- C4(NAD^+ , native) (Å)
None	NAD^+	34	2.9	4.2	-
	s NAD^+	47	3.4 ^a	3.9 ^a	0.2
	ac ³ PdAD ⁺	6.5	2.9	4.4	0.4
	fPdAD ⁺	9	2.9	5.1	0.6
Val292Gly	NAD^+	51	2.9	4.2	0.1
	s NAD^+	65	3.5 ^a	4.0 ^a	0.4
	ac ³ PdAD ⁺	9	3.1	4.3	0.4
	fPdAD ⁺	9	2.9	4.3	0.4
Ala317Gly	NAD^+	40	2.8	4.0	0.1
	s NAD^+	34	3.4 ^a	4.0 ^a	0.2
	ac ³ PdAD ⁺	18	2.9	4.1	0.4
	fPdAD ⁺	5	2.9	4.7	0.4
Phe319Gly	NAD^+	33	2.9	4.2	0.2
	s NAD^+	21	3.4 ^a	4.0 ^a	0.4
	ac ³ PdAD ⁺	15	3.0	4.2	0.4
	fPdAD ⁺	5	2.8	4.9	0.1

^a Instead of oxygen, s NAD^+ has a sulphur atom bound in the side chain of the pyridinium ring.

In the Val292Gly mutant NAD^+ and sNAD^+ exhibit a similar increase of the "out-of-plane" rotation, whereas with ac^3PdAD^+ and fPdAD^+ this value has not changed significantly. However, in the case of fPdAD^+ the positioning of the pyridinium ring has somewhat improved compared to the native enzyme.

Also the NAD^+ analogue geometries have been simulated in the Ala317Gly and Phe319Gly mutants since Ala 317 and Phe 319 are, like Val 292, hydrogen bonded to the carboxamide side chain. Relevant information is contained in table 7.IV.

Although only a small increase of the NAD^+ "out-of-plane" rotation is observed with the Ala317Gly mutant, ϕ has increased two-fold with ac^3PdAD^+ . The "out-of-plane" values of the other analogues sNAD^+ and fPdAD^+ have been affected adversely, whereas their pyridinium positions do not differ that much. The positive effect of the mutation on ac^3PdAD^+ can be explained by the fact that the methyl group of ac^3PdAD^+ in the native enzyme is hindered sterically, whereas reduction of the size of the amino acid residue gives more space in the active site to position the methyl group more favourably. It is interesting to note that in the Val292Gly mutant ac^3PdAD^+ is not affected, despite the fact that both Val 292 and Ala 317 are hydrogen bonded to the amide group of the side chain.

With regard to the Phe319Gly mutant, rather drastic effects are observed with sNAD^+ and fPdAD^+ . In contrast with NAD^+ , sNAD^+ shows a large decrease of ϕ . Compared to the native enzyme, the position of the pyridinium ring of fPdAD^+ has improved substantially.

In an attempt to get more insight into the influence of Val 292 on the coenzyme geometry, also substitutions of Val 292 to alanine and isoleucine were simulated with the less active coenzyme analogue fPdAD^+ . However, only very small differences could be observed.

7.4 Conclusions

The AMBER model enables us to study the effects of amino acid substitutions in the active site on the coenzyme geometry and corresponding activity. Due to their influence on the coenzyme positioning Val 292, Ala 317, Phe 319 and Arg 369 seem to be first choice candidates for site-directed mutagenesis of HLADH in order to verify the correctness of our approach.

References

1. Van de Goor-Kucerová, J., Kocken, H.J.M., Sluyterman, L.A.AE. and Meijer, E.M. *Nucleic Acid Research*, submitted for publication.
2. Eklund, H. and Brändén, C.I. in "Coenzymes and Cofactors, Pyridine nucleotide coenzymes" (D. Dolphin, O. Avramovic and R. Poulson, eds.), John Wiley and Sons, New York 2A (1987), 51-98.
3. Jörnvall, H., Eklund, H. and Brändén, C.I. *J. Biol. Chem.* 253 (1978), 8414-8419.
4. Weiner, P.K and Kollman, P.A. *J. Comp. Chem.* 2 (1981), 287-303.
5. Benner, S.A. *Redesigning the molecules of life* (1988), 115-175.
6. Plapp, B.V., Ganzhorn, A.J., Gould, R.M., Green, D.W. and Hershey, A.D. *Prog. Clin. Biol. Res.* 232 (1987), 227-236.
7. Ganzhorn, A.J. and Plapp, B.V. *J. Biol. Chem.* 263 (1988), 5446-5454.

APPENDIX A

Added parameters of AMBER

<i>NAD</i> ⁺				<i>m</i> ⁴ <i>NAD</i> ⁺			
Bond stretching				Bond stretching			
A1-A2	K_R	R_{eq}		A1-A2	K_R	R_{eq}	
CD-N*	448	1.38		CA-CT	317	1.51	
CA-C	317	1.57		CA-CA	469	1.39	
Bond bending				Bond bending			
A1-A2-A3	K_θ	θ		A1-A2-A3	K_θ	θ	
CD-N*-CD	70	121.2		CD-CA-CT	70	120.0	
CD-CD-N*	70	121.2		CD-CA-CA	85	120.0	
CD-CA-C	58	115.1		CA-CT-HC	35	109.9	
CA-C-O	80	119.8		CA-CA-C	85	120.0	
CA-C-N	70	115.7		CT-CA-CA	70	120.0	
CA-CD-N*	70	119.5		Torsional			
P-OS-P	100	132.9		A1-A2-A3-A4	$V_n/2$	γ	n
CD-N*-CH	70	120.6		X-CT-CA-X	0.0	0.0	2
Torsional				X-CA-CA-X	5.3	180.0	2
A1-A2-A3-A4	$V_n/2$	γ	n	<i>sNAD</i> ⁺			
X-N*-CD-X	6.6	180.0	2	Bond stretching			
X-CA-C-X	5.3	180.0	2	A1-A2	K_R	R_{eq}	
<i>ac</i> ³ <i>PdAD</i> ⁺ , <i>pp</i> ³ <i>PdAD</i> ⁺				C-SD	328	1.71	
Bond bending				SD-LP	600	0.68	
A1-A2-A3	K_θ	θ		Bond bending			
CA-C-CT	85	120.0		A1-A2-A3	K_θ	θ	
C-CT-HC	35	109.5		CA-C-SD	64	121.2	
C-CT-CT	63	111.1		SD-C-N	64	123.7	
CT-CT-HC	35	109.5					
HC-CT-HC	36	109.5					

(continuation of sNAD ⁺)				Bond bending		
C-SD-LP	600	96.7		A1-A2-A3	K _θ	θ
LP-SD-LP	600	160.0		CA-C-H	35	120.1
Torsional				O-C-H	35	120.1
A1-A2-A3-A4	V _n /2	γ	n	<i>DMSO</i>		
X-CA-C-X	5.3	180.0	2	Bond stretching		
X-C-SD-X	1.0	0.0	3	A1-A2	K _R	R _{eq}
<i>cn</i> ³ PdAD ⁺				O-S	525	1.48
Bond stretching				S-C3	222	1.81
A1-A2	K _R	R _{eq}		Bond bending		
CA-C'	444	1.42		A1-A2-A3	K _θ	θ
C'-N'	720	1.16		O-S-C3	68	107.6
Bond bending				C3-S-C3	62	98.9
A1-A2-A3	K _θ	θ		<i>Zinc</i>		
CD-CA-C'	85	119.4		Symbol	Radius (Å)	Welldepth kcal.mol ⁻¹
CA-C'-N'	70	180.0		Zn	1.48	0.05
<i>clac</i> ³ PdAD ⁺						
Bond stretching						
A1-A2	K _R	R _{eq}				
CT-CL	465	1.78				
Bond bending						
A1-A2-A3	K _θ	θ				
HC-CT-CL	77	106.9				
C-CT-CL	82	111.3				
<i>fp</i> PdAD ⁺						
Bond stretching						
A1-A2	K _R	R _{eq}				
C-H	331	1.05				

APPENDIX B

The full names of the core of amino acids introduced in the model are:

1. Cys 46	23. Gly 204
2. Arg 47	24. Val 222
3. Ser 48	25. Asp 223
4. His 51	26. Ile 224
5. Thr 56	27. Asn 225
6. Leu 57	28. Lys 228
7. His 67	29. Val 268
8. Glu 68	30. Ile 269
9. Phe 93	31. Arg 271
10. Thr 94	32. Thr 274
11. Leu 116	33. Ile 291
12. Phe 140	34. Val 292
13. Leu 141	35. Gly 293
14. Gly 173	36. Val 294
15. Cys 174	37. Pro 295
16. Gly 175	38. Gly 316
17. Thr 178	39. Ala 317
18. Ser 182	40. Ile 318
19. Leu 200	41. Phe 319
20. Gly 201	42. Gly 320
21. Gly 202	43. Leu 362
22. Val 203	44. Arg 369

SUMMARY

This thesis deals with the results of chemical and enzymatic studies on the coenzyme NAD^+ and its reduced form NADH . In combination with specific enzymes (dehydrogenases) the coenzyme is involved in the reversible stereospecific dehydrogenation of many substrates.

Although the syntheses of optically pure compounds are becoming increasingly important, the number of successful industrial applications of NAD^+ -dependent enzymes is limited so far. Much research is in progress to increase the use of NAD^+ -dependent enzymes, but, up till now, no clear insight is obtained into the relationship between structure and function of enzyme and coenzyme, i.e., no systematic explanation and interpretation of activity and stereoselectivity have been provided so far. This thesis is aiming at improving our fundamental insight into the interaction of enzyme and coenzyme.

Insight into the enzymatic mechanism can be gained by using NADH model systems. Donkersloot and Buck postulated in 1981 that, among other factors, the rate of the hydride-transfer reactions with NAD^+/NADH is caused by the fact that in the kinetic step an "out-of-plane" orientation of the carboxamide group occurs (i.e., the rotation of the carboxamide group out of the pyridinium plane). They found, according to quantum chemical calculations that the enthalpy of the transition state of the hydride-transfer is lowered when the carboxamide is rotated out of the pyridinium plane. This is confirmed by röntgen data from complexes of NAD^+ with horse liver alcohol dehydrogenase (HLADH) and with glyceraldehyde-3-phosphate dehydrogenase (GAPDH); both showing carbonyl "out-of-plane" orientations.

The concept of the carbonyl "out-of-plane" orientation is verified experimentally using a NADH model compound in which the carboxamide group is rotated permanently out of the pyridinium plane. The NADH model is studied as an efficient catalyst in the stereospecific reduction of benzoin (Chapter 2). A highly asymmetric induction is obtained by the intermediacy of a coordinated complex of substrate, NADH model compound and Mg^{2+} ions. The *R*- and *S*- NADH model compounds turned out to be highly enantioselective towards *S*- and *R*-benzoin, respectively. This remarkable selectivity should allow an efficient kinetic resolution of benzoin.

To obtain more insight into the orientation of the coenzyme within the complex of enzyme, coenzyme and substrate, the geometry of NAD^+ analogues in HLADH is studied and related to activity. The geometry of NAD^+ and NAD^+ derivatives (modified in the pyridinium side chain) in the active site of HLADH is simulated using

AMBER molecular mechanics calculations (Chapter 3). Starting point is a 3D structure of the ternary complex of HLADH, NAD^+ and the pseudo substrate dimethyl sulfoxide (DMSO). The method proved to be a useful tool for describing the influence of side chain substitutions on the coenzyme geometry in the ternary complex.

In order to relate the activity of NAD^+ analogues to their conformation in the active site of HLADH, kinetic experiments with the substrate isopropanol were carried out (Chapter 4). With isopropanol the hydride-transfer is the rate-limiting step. It seems that the measured enzymatic activities of the analogues can be rationalized by their conformation in the active site as determined with AMBER molecular mechanics taking into account their intrinsic reactivities. Particularly the magnitude of the "out-of-plane" rotation of the carboxamide side chain is determining.

Using our molecular mechanics model we also studied the conformational changes in HLADH upon binding of NAD^+ and NAD^+ fragments (Chapter 5). In the absence of NAD^+ the enzyme conformation differs substantially from the one found in the active complex of enzyme, coenzyme and substrate. The simulation studies with NAD^+ fragments show further that the adenosine part of NAD^+ is essential in inducing the required conformational change to bring the enzyme in its active form.

An example of the commercial use of NAD^+ -dependent dehydrogenases is the continuous production of L-amino acids from the corresponding keto acids in a membrane reactor using NAD^+ bound to polyethylene glycol (PEG- NAD^+). Surprisingly the dehydrogenase is nearly fully active with PEG- NAD^+ . Chapter 6 reports that the AMBER molecular mechanics model enables us to rationalize the observed enzymatic activity in the presence of PEG- NAD^+ .

Although the major part of this thesis is focussed on modelling of the coenzyme, the relation between enzyme and coenzyme can also be elucidated by modifying the enzyme structure in its active site. Using molecular mechanics, a number of mutated HLADH's have been simulated in order to select those amino acid residues which substantially affect the coenzyme geometry (Chapter 7). The methodology developed may be helpful in selecting targets for site-directed mutagenesis in order to engineer genetically HLADH so as to optimize the interaction of the apo-enzyme and coenzyme. Obviously in the near future molecular dynamics studies are the preferred method in order to obtain more detailed information.

SAMENVATTING

Het onderzoek dat in dit proefschrift wordt beschreven, betreft een chemische en enzymatische studie aan het coënzym NAD^+ en zijn gereduceerde vorm NADH . In combinatie met specifieke enzymen (dehydrogenases) is het coënzym betrokken bij de reversibele stereospecifieke dehydrogenatie van vele substraten.

Hoewel de synthese van optisch zuivere verbindingen steeds belangrijker wordt, is het aantal succesvolle industriële toepassingen van NAD^+ -afhankelijke enzymen nog beperkt. Momenteel wordt veel onderzoek gedaan naar verhoging van het gebruik van NAD^+ -afhankelijke enzymen. Tot nu toe is echter nog geen duidelijk inzicht verkregen in de relatie tussen structuur en functie van enzym en coënzym, d.w.z. systematische verklaringen voor activiteit en stereoselectiviteit zijn niet voorhanden. Dit proefschrift beoogt het fundamentele inzicht in de interactie van het enzym met het coënzym te verhogen.

Inzicht in het enzymatische werkingsmechanisme kan o.a. worden verkregen door gebruik te maken van NADH modelsystemen. Door Donkersloot en Buck is in 1981 gepostuleerd dat de snelheid van hydride-overdrachtsreacties met NAD^+/NADH mede wordt veroorzaakt doordat in de kinetische stap een "out-of-plane" oriëntatie van de NAD^+ carbonamide groep optreedt (d.w.z. het uit het pyridiniumvlak gedraaid zijn van de carbonamide groep). Gebruikmakend van kwantumchemische berekeningen toonden zij aan dat door draaiing van de carbonamide groep uit het vlak van de pyridiniumring een overgangstoestand wordt doorlopen die energetisch gunstiger is dan in het geval dat er geen "out-of-plane" oriëntatie optreedt. Dit wordt bevestigd door röntgenkristallografische gegevens van complexen van paardelever alcoholdehydrogenase (HLADH) en glyceraldehyde-3-fosfaatdehydrogenase (GAPDH) met NAD^+ . In beide gevallen wordt inderdaad een carbonyl "out-of-plane" oriëntatie waargenomen.

Het concept van de carbonyl "out-of-plane" oriëntatie is verder geverifieerd aan de hand van een modelverbinding van NADH waarbij de carbonamidegroep door zijgroepen aan de pyridinering permanent uit het vlak is gedraaid. De NADH modelverbinding is bestudeerd als een efficiënte katalysator in de stereospecifieke reductie van benzoïne (Hoofdstuk 2). Een hoge asymmetrische inductie wordt verkregen door de opbouw van een gekoördineerd complex van substraat, NADH modelverbinding en Mg^{2+} ionen. Gebleken is dat de *R*- en *S*- NADH modelverbindingen opmerkelijk enantioselectief zijn t.o.v. respectievelijk *S*- en *R*-benzoïne. Op deze wijze is de NADH modelverbinding tevens bruikbaar voor een efficiënte kinetische resolutie.

Om meer inzicht te verkrijgen in het belang van de oriëntatie van het coënzym binnen het complex van enzym, coënzym en substraat is de geometrie van NAD^+ en analoga in het HLADH bestudeerd en gerelateerd aan de activiteit.

De geometrie van NAD^+ en NAD^+ derivaten (gemodificeerd in de zijketen van de pyridiniumring) in de actieve holte van het alcoholdehydrogenase is gesimuleerd met AMBER moleculaire mechanica berekeningen (Hoofdstuk 3). Hierbij is uitgegaan van een 3D structuur van het ternaire complex van HLADH/ NAD^+ met het pseudosubstraat dimethylsulfoxide (DMSO). Het blijkt dat de methode in staat is de invloed van de zijketen-substituties op de coënzymgeometrie in het ternaire complex te beschrijven.

Om een relatie te leggen tussen de activiteit van de NAD^+ analoga en hun konformatie in de actieve holte van HLADH zijn kinetische experimenten met het substraat isopropanol uitgevoerd (Hoofdstuk 4). Met isopropanol is de hydride-overdracht de snelheidsbepalende stap. Gebleken is dat de zo gemeten enzymatische activiteit van de analoga kan worden verklaard d.m.v. hun konformatie in de actieve holte zoals bepaald met AMBER moleculaire mechanica berekeningen, rekening houdend met de intrinsieke reactiviteit. Met name de grootte van de "out-of-plane" rotatie van de carbonamide zijgroep is bepalend.

Met behulp van het opgestelde moleculaire mechanica model is ook een studie verricht naar de konformatieverandering die het HLADH ondergaat bij binding van NAD^+ en NAD^+ fragmenten (Hoofdstuk 5). In afwezigheid van NAD^+ werd een andere enzymkonformatie gevonden dan in het actieve complex van enzym, coënzym en substraat. Bij de bestudering van NAD^+ fragmenten is verder naar voren gekomen dat het adenosinegedeelte van NAD^+ van essentieel belang is voor de vereiste konformatieverandering van het enzym.

Een voorbeeld van het commercieel gebruik van NAD^+ -afhankelijke dehydrogenases is de continue productie van L-aminozuren uit de overeenkomstige ketozuren m.b.v. een membraanreaktor waarbij NAD^+ gebonden is aan polyethyleenglycol (PEG- NAD^+). Op zich is het verrassend dat het dehydrogenase vrijwel volledig actief is met PEG- NAD^+ . Hoofdstuk 6 beschrijft dat het AMBER moleculaire mechanica model ons in staat stelt om de waargenomen enzymatische activiteit in aanwezigheid van PEG- NAD^+ te verklaren.

Hoewel het grootste gedeelte van het proefschrift is gewijd aan modelstudies met het coënzym, kan de relatie tussen enzym en coënzym ook worden opgehelderd door de enzymstructuur in zijn actieve holte te modificeren. Op basis van moleculaire mechanica modellering is een aantal gemuteerde HLADH's gesimuleerd om na te gaan welke enzymmodificaties (aminozuursubstituties) in het HLADH de coënzymgeometrie beïnvloeden (Hoofdstuk 7). De ontwikkelde methode kan van nut zijn bij het selecteren

van gewenste puntmutaties in HLADH. Uiteraard zullen in de nabije toekomst moleculaire dynamica berekeningen de meest aangewezen weg zijn om de verkregen inzichten verder te detailleren.

CURRICULUM VITAE

De schrijfster van dit proefschrift werd geboren op 16 juni 1964 in Geldrop. Ze behaalde het VWO diploma in 1982 aan het Rythovius College in Eersel. In dat zelfde jaar is ze begonnen met de studie Scheikundige Technologie aan de Technische Universiteit Eindhoven. Het afstudeerwerk werd verricht bij de vakgroep Instrumentele Analyse, en in 1986 werd het ingenieursdiploma behaald. Aansluitend startte ze met de tweejarige Tweede Fase Onderzoekersopleiding bij de vakgroep Organische Chemie. Na de afronding in 1988, werd het onderzoek hiervan voortgezet als promotieonderzoek gesubsidieerd vanuit het IOP-koolhydraten.

NAWOORD

Graag wil ik iedereen hartelijk bedanken die, op welke wijze dan ook, heeft bijgedragen aan de totstandkoming van dit proefschrift. Dit geldt in het bijzonder voor mijn eerste promotor, prof. dr. E.M. Meijer, voor zijn begeleiding en zijn immer aanwezige enthousiasme en optimisme. Prof. dr. L.A.AE. Sluyterman wil ik heel hartelijk bedanken voor de vele discussies en zijn waardevolle raadgevingen waardoor het onderzoek aan diepte heeft gewonnen. Ook wil ik prof. dr. H.M. Buck bedanken voor zijn aandeel in het onderzoek dat ten grondslag ligt aan dit proefschrift, en prof. dr. R.M. Kellogg voor het aanvaarden van het tweede promotorschap en het kritisch doorlezen van het proefschrift.

Naast alle medewerkers van de vakgroep Organische Chemie, waarbinnen het uiteindelijke werk is verricht, wil ik met name dr. Jef Vekemans en dr. ir. Peter de Kok bedanken voor hun belangrijke bijdragen en ondersteuning.

Verder ben ik ook veel dank verschuldigd aan het CAOS/CAMM centrum in Nijmegen voor het ter beschikking stellen van de computerprogramma's voor het uitvoeren van de AMBER berekeningen.

Als laatste dank ik al diegenen die tijdens de afgelopen jaren hun belangstelling hebben getoond.

Bedankt,

Nicoline

STELLINGEN

behorende bij het proefschrift

**"NAD⁺-NADH MODELLING STUDIES
AN ENZYMATIC AND CHEMICAL APPROACH"**

1. Het feit dat de alcohol dehydrogenases van *Drosophila melanogaster* en paardelever tot éénzelfde sub-sub-klasse worden gerekend doet weinig recht aan de essentiële verschillen tussen beide enzymen.

Alleman, R.K., Hung, R. en Benner, S.A. *J. Am. Chem. Soc.* **110** (1988), 5555-5560.
Jörmvall, H., Persson, M. en Jeffery, J. *Proc. Nat. Acad. Sci. U.S.A.* **78** (1981), 4226-4230.

Enzyme Nomenclature. Recommendations (1978), Academic Press, New York.

2. De wijze van binding van AMP in de actieve holte van HLADH bevestigt de essentiële rol die het adenosinegedeelte van NAD^+ speelt bij de konformatieverandering van HLADH.

Sicsic, S., Durand, P., Langrené, S. en Le Goffic, F. *FEBS Lett.* **176** (1984), 321-324
en *Eur. J. Biochem.* **155** (1986), 403-407.

Dit proefschrift, hoofdstuk 5.

3. De energiekurve voor de torsiehoekdraaiing van de NAD^+ -carbonamidegroep berekend door Perahia et al. is onbetrouwbaar.

Perahia, D., Pullman, B. en Saran, A. in "Structure and conformation of nucleic acids and protein-nucleic acid interactions", M. Sundaralingam en S.T. Rao (eds.), University Park Press, Baltimore MD, (1975), 685-708.

Cummins, P.L. en Gready, J.E. *J. Mol. Struct. (Theochem)* **183** (1989), 161-174.

4. De bepaling van de vormingswarmte van NAD^+ (en analoga) als functie van de torsiehoekdraaiing van de NAD^+ -carbonamidegroep (en analoga) m.b.v. MNDO levert een onjuist resultaat.

Donkersloot, M.C.A. en Buck, H.M. *J. Am. Chem. Soc.* **103** (1981), 6554-6558.

5. Het voorgestelde ternaire complex voor de verklaring van de stereoselectieve reductie van benzoïne is niet in tegenspraak met de Regel van Cram.

Dit proefschrift, hoofdstuk 2.

Sykes, P. "A guidebook to mechanism in organic chemistry", 5e ed., Longman, London, (1981), 230-232.

6. Bij het vergelijken van resultaten waarbij gebruik is gemaakt van verschillende versies van computerprogramma's is voorzichtigheid geboden.
7. De kracht van computer-modellering ligt in de strukturopheldering van beperkte makro-moleculaire modificaties waarvan geen röntgenstructuren bekend zijn. Hierdoor kunnen experimentele resultaten worden verklaard, inzichten worden verbeterd en nieuwe ideeën worden gegenereerd.

Dit proefschrift, hoofdstuk 3 t/m 7.

8. Het is verbazingwekkend dat de regeling van kwaliteitsbewaking in de ziekenhuizen achterblijft bij die van de industrie.
9. Bij het mislukken van experimenten gaat het motto "soms is meestal altijd" helaas maar al te vaak op.
10. Gelet op de mobiliteit die ingebakken is in het westerse cultuurpatroon zal de afstemming van het openbaar vervoer op deze mobiliteitsbehoefte geen voordeel opleveren voor het milieu.